# Sparse and Decoupling Control Strategies based on Takagi-Sugeno Fuzzy Models

Qianfang Liao and Da Sun

***Abstract*—In order to better handle the coupling effects when controlling multiple-input multiple-output (MIMO) systems, taking the decentralized control structure as the basis, this paper proposes a sparse control strategy and a decoupling control strategy. Type-1 and type-2 Takagi-Sugeno (T-S) fuzzy models are used to describe the MIMO system, and the relative normalized gain array (RNGA) based criterion is employed to measure the coupling effects. The main contributions include: i). compared to the previous studies, a manner with less computational cost to build fuzzy models for the MIMO systems is provided, and a more accurate method to construct the so-called effective T-S fuzzy model (ETSM) to express the coupling effects is developed; ii). for the sparse control strategy, four indexes are defined in order to extend a decentralized control structure to a sparse one. Afterwards, an ETSM-based method is presented that a sparse control system can be realized by designing multiple independent single-input single-output (SISO) control-loops; iii). for the decoupling control strategy, a novel and simple ETSM-based decoupling compensator is developed that can effectively compensate for both steady and dynamic coupling effects. As a result, the MIMO controller design can be transformed to multiple non-interacting SISO controller designs. Both of the sparse and decoupling strategies allow to use linear SISO control algorithms to regulate a closely coupled nonlinear MIMO system without knowing its exact mathematical functions. Two examples are used to show the effectiveness of the proposed strategies.**

***Index Terms*—effective fuzzy model, T-S fuzzy model, sparse control, decoupling control, type-2 fuzzy logic.**

## I. Introduction

Due to the existence of coupling effects, the controller design for multiple-input multiple-output (MIMO) system is generally of much more complexity when compared to its single-input single-output (SISO) counterpart. In the area of MIMO control, although different sophisticated schemes have been proposed, decentralized control remains popular since it employs the simplest control structure that one manipulated variable (system input) regulates only one controlled variable (system output), which is convenient to tune, maintain and implement [1]-[3]. In general, there are two steps for decentralized control to handle coupling effects: first, the inputs and outputs are carefully paired that the resulting one-for-one control structure is of minimum coupling effects among the pairs; second, proper algorithms are used to design and tune the sub-controllers of the paired input-output channels to eliminate the coupling effects and achieve desired performance. For the first step, different interaction measures are available for pairing, such as the controllability and observability gramians [4]-[7], and the relative gain array (RGA) family [1]-[3],[8]-[12]. For the second step, a challenge exists that the sub-controller design generally requires to know the coupling information [12]. In many existing studies of the model-based decentralized control, extra terms are added to the model of isolated paired channel to characterize the coupling effects for sub-controller design [3]. These extra terms may not be always obtainable, especially in a complex MIMO system. An alternative, called "effective model" [12]-[15], is proposed that the coefficients of the isolated paired channels' models are revised to express the coupled results. In [15], the effective Takagi-Sugeno (T-S) fuzzy models (ETSMs) is presented, where the coefficients of the T-S fuzzy model are revised according to the coupling effects measured by the relative normalized gain array (RNGA) based criterion [2]. Unlike the effective transfer functions in [12]-[14], ETSM [15] can be used when the exact mathematical system functions are not available, and is more robust against the uncertainties. In addition, it allows to apply linear SISO control algorithms on the decentralized controller design for nonlinear MIMO systems thanks to the fact that T-S fuzzy model is composed of a group of linear local models [16].

However, when there are strong coupling effects among the paired input-output channels, it is possible that no decentralized control yields a satisfactory performance due to the limited flexibility of control structure. On the other hand, centralized controller using full-dimensional control structure that each output is regulated by all inputs can handle the strong coupling effects, but can result in greatly increased complexity and cost in controller design and tuning, especially when the MIMO system is of high dimension. For this problem, one solution is to increase the flexibility of the control structure, beyond the one-for-one, to the extent that a satisfactory result can be achieved without necessarily using full-dimensional control structure. Sparse control, which is a compromise between decentralized and centralized control, is introduced as this solution [5]-[7],[11],[14]. In sparse control, part of the outputs are regulated by more than one inputs, thus it has extra design degree of freedom to manage the coupling effects compared to the decentralized control, and requires less computational cost compared to the centralized control. In [5]-[7], the methods to select sparse control structure using gramian-based interaction measure and based on linear/bilinear/nonlinear mathematical models are given. These methods have not referred to sparse controller design and not shown any sparse control performance. In [14], a scheme using RNGA and effective transfer function to determine sparse control structure and design sparse

Q. Liao and D. Sun are with the Center for Applied Autonomous Sensor Systems (AASS), Örebro University, 702 81, Sweden (Corresponding author: Da Sun). E-mail: Qianfang.Liao@oru.se; Da.Sun@oru.se

This work was supported by Semantic Robots Research Profile, funded by the Swedish Knowledge Foundation (KKS).

controller is presented. This scheme is based on linear transfer functions and may not work for nonlinear systems. In [11], a method based on T-S fuzzy model to select sparse control structure is proposed. This method works for both linear and nonlinear systems, and does not require to know the exact mathematical system functions. However, it does not investigate detailed sparse control strategy.

Another solution to handle the closely coupled pairs is to insert a decoupling compensator into the control-loop to compensate for the coupling effects and subsequently decouple the paired channels, such that the decentralized controller can be decomposed to multiple non-interacting SISO controllers. Different methods have been proposed in this area. A static decoupling compensator in [17] is given for decoupling at low frequencies, and the dynamic decoupling compensator in [18]-[23] can work in a wider range of frequency. However, the dynamic compensators may result in greatly increased complexity in the compensator itself or in the decoupled MIMO system. The methods in [17]-[23] are designed for linear systems. For nonlinear systems, several intelligent decoupling schemes can be found. In [24], a static neural network is used to construct an inverse system for decoupling, and then the controller is designed based on the pseudo linear transfer functions. In [25], a hybrid fuzzy decoupling method is developed based on the linearized systems and using the fuzzy logic to approximate the nonlinear coupling effects. In [26], by using RGA to select the pairs, a decoupling control law is proposed for a $2 \times 2$ system expressed by a linear function with nonlinear terms, and the adaptive neural-fuzzy inference system is used to estimate the nonlinear term. RGA only uses the steady-state gains for interaction measure and may give incorrect results because of lacking dynamic information. It is worth noting that the implement of these methods requires the knowledge of the systems' mathematical functions to a certain extent. In [27], a fuzzy decoupling control system is presented where Mamdani fuzzy logic is used. Mamdani fuzzy logic may not be sufficient to describe the system dynamics and generally needs more fuzzy rules when compared to T-S fuzzy logic [28].

Given the aforementioned condition, for a MIMO nonlinear system with closely coupled input-output channels and without knowing its exact mathematical functions, in order to achieve desired performance without applying full centralized control, practical strategies are needed to provide further improvement based on decentralized controllers. In this paper, using T-S fuzzy models to describe the MIMO system, and using RNGA which considers both steady and dynamic information to measure the coupling effects, a sparse control strategy and a decoupling control strategy are developed. Both type-1 and type-2 fuzzy logic are investigated for the proposed strategies. Compared to the type-1 (traditional) fuzzy model using crisp fuzzy membership grades, type-2 fuzzy model possesses increased fuzziness in the fuzzy membership grades. As a result, it has additional power to describe the uncertainties and can be more robust against the noise and disturbance [29]-[33]. The contributions of this paper are summarized as follows.

- Compared to the previous studies in [3],[11],[15], improvement is made in terms of fuzzy model construction. Subsequently, the cost for MIMO system modeling and the online computational complexity for the fuzzy model based controllers can be reduced. In addition, compared to the study in [15], a more accurate ETSM calculation is developed to provide a better expression for the coupled results on both steady and dynamic properties.
- For the sparse control strategy, four indexes are defined from the RNGA based interaction measure to select the sparse control structure, and an ETSM-based method is presented that the sparse controller for a nonlinear MIMO system can be achieved by designing multiple independent SISO controllers using linear algorithms.
- For the decoupling control strategy, using the information provided by RNGA, a T-S fuzzy model based decoupling compensator is proposed which can effectively compensate for both steady and dynamic coupling effects to decouple the paired channels, and subsequently offload the burden on decentralized control. Unlike the existing methods [24]-[26], this decoupling compensator can be derived and implemented without the priori-knowledge of exact mathematical functions or linearized functions of the system. While compared to the Mamdani fuzzy logic based decoupling method in [27], the proposed method is based on T-S fuzzy model that can better describe the system dynamics, and provides a platform to apply linear SISO control algorithms on the regulation of strongly coupled nonlinear MIMO systems.

Two nonlinear multivariable systems are employed to show and compare the performances of the proposed strategies, as well as that of type-1 and type-2 fuzzy models. The results demonstrate that by using the same SISO control algorithm in the sub-controller designs, both sparse and decoupling control outperform their decentralized counterpart, and the decoupling control achieves better output responses than the sparse control does. In addition, type-2 fuzzy system achieves more robust performance compared to its type-1 counterpart, which is more evident when larger uncertainty appears.

*Notations*: $I_{m\times n}$ and $0_{m\times n}$ denote the $m \times n$ identity matrix and $m \times n$ zero matrix, respectively; $\|\cdot\|$ means Euclidean norm; $A = [a(i,j)]_{n\times n}$ is an $n \times n$ matrix, where $a(i,j)$, a variable or a function with the subscripts composed by "$i$" or/and "$j$", denotes the element in $A$. The subscript combinations indicate the positions of the elements in the $n \times n$ matrix as follows: i). $*_{ij}$ and $*_{ji}$ mean the elements in $i$th row and $j$th column; ii). $*_{ii}$ or $*_{jj}$ means the elements in $i$th or $j$th row and $i$th or $j$th column; iii). $*_i$ or $*_j$ means it exists in all the elements of $i$th row or $j$th column.

## II. Preliminaries

In this section, some preliminary works, including the RNGA based criterion and the ETSM based decentralized control strategy, are introduced. These works are the basis of our study. The following assumption is applied throughout this paper.

**Assumption 1**: The MIMO systems considered in this paper are square in dimension, open-loop stable, and non-singular in steady-state conditions. The time delays between inputs and

outputs are constant and measurable, and for each input, the delays between it and all outputs are considered to be identical.

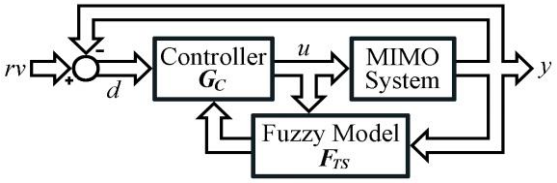


Fig. 1. T-S fuzzy model based control-loop for a MIMO system

A T-S fuzzy model based control-loop for an $n \times n$ MIMO system is shown in Fig. 1, where $rv = [rv_1 \cdots rv_n]^T \in \mathbb{R}^n$ stand for reference values, $u = [u_1 \cdots u_n]^T \in \mathbb{R}^n$ are system inputs, $y = [y_1 \cdots y_n]^T \in \mathbb{R}^n$ are system outputs, and $d = rv - y$; $F_{TS} = \left[f_{TS,ij}\right]_{n\times n}$ is a $n \times n$ T-S fuzzy model matrix to describe the MIMO system, $f_{TS,ij}$ is the T-S fuzzy model (SISO) for isolated channel $y_i - u_j$ ($i,j = 1,\cdots,n$); $G_C = \left[g_{C,ij}\right]_{n\times n}$ is the MIMO controller.

When designing a decentralized controller $G_C$, the primary step is to select the dominant input-output pairs to form a decentralized control structure. For this issue, the RNGA based criterion is a helpful means [2],[3],[11],[15]. For a MIMO system represented by $F_{TS}$, RNGA based criterion uses the steady-state gain, $\hbar_{ij}$, and the normalized integrated error, $e_{ij}$, of each $f_{TS,ij}$ to evaluate the coupling effects and then pick out the dominant elements [3],[11],[15]. Collecting $\hbar_{ij}$s and $e_{ij}$s of all elements in $F_{TS}$, we can have two matrices, $\mathcal{K} = \left[\hbar_{ij}\right]_{n\times n}$ and $\mathcal{E} = \left[e_{ij}\right]_{n\times n}$. Afterwards, the RGA and RNGA for $F_{TS}$ can be calculated by the following equations [2],[3],[11],[15]:

$$RGA = \left[\lambda_{ij}\right]_{n\times n} = \mathcal{K} \otimes (\mathcal{K})^{-T} \quad (1)$$

$$RNGA = \left[\phi_{ij}\right]_{n\times n} = (\mathcal{K} \odot \mathcal{E}) \otimes (\mathcal{K} \odot \mathcal{E})^{-T} \quad (2)$$

where $\otimes$ and $\odot$ are element-by-element product and division, respectively, $(\cdot)^{-T}$ means inverse and transpose matrix. Note that the sum of the elements in each row/column of RGA or RNGA is 1. The definitions of the relative gain $\lambda_{ij}$ and the relative normalized gains $\phi_{ij}$ are [1]-[3]:

$$\begin{cases} \lambda_{ij} = \hbar_{ij} / \hat{\hbar}_{ij} \\ \phi_{ij} = \frac{\hbar_{ij}/e_{ij}}{\hat{\hbar}_{ij}/\hat{e}_{ij}} = \frac{\hbar_{ij}}{\hat{\hbar}_{ij}} \cdot \frac{\hat{e}_{ij}}{e_{ij}} = \lambda_{ij} \cdot \gamma_{ij} \end{cases} \quad (3)$$

where $\gamma_{ij} = \hat{e}_{ij}/e_{ij}$ is called relative normalized integrated error, $\hat{\hbar}_{ij}$ and $\hat{e}_{ij}$ are the apparent steady-state gain and normalized integrated error of $y_i - u_j$ when other loops are closed (the closure of other loops can cause the coupling effects on $y_i - u_j$). From (3), we can know that when $\lambda_{ij}$ and $\phi_{ij}$ are close to 1 (i.e., the values of $\hat{\hbar}_{ij}$ and $\hat{e}_{ij}$ are close to $\hbar_{ij}$ and $e_{ij}$, respectively), the channel $y_i - u_j$ is highly independent (dominant) and robust to the coupling effects caused by other channels. Subsequently, $y_i - u_j$ is likely to be selected as a pair. The pairing rules of the RNGA based criterion are presented as follows [2],[3],[11],[15]:

i). *$\lambda_{ij}$s and $\phi_{ij}$s of the paired channels should be positive*;

ii). *$\phi_{ij}$s of the paired channels should be closest to 1*;

iii). $NI = \frac{det(\mathcal{K})}{\prod_{i=1}^{n} \hbar_{ii}} > 0$, *NI is the Niederlinski index* [34].

where $\det(\mathcal{K})$ is the determinant of $\mathcal{K}$ after column swapping to place the paired elements in the diagonal positions if necessary, and $\prod_{i=1}^{n} \hbar_{ii}$ is the product of steady-state gains of the paired channels. A positive NI is a necessary condition for a stable control system [1]-[3],[11]-[15].

In [15], a decentralized control strategy based on RNGA criterion and T-S fuzzy model is proposed. We briefly introduce it as follows:

i). By using RNGA based criterion, the inputs and outputs are paired to determine a nominal fuzzy model matrix, denoted by $\bar{F}_{TS}$, which keeps the paired elements of $F_{TS}$ and discards the rest. For instance, a $3 \times 3$ system with pairing structure $y_1 - u_3/y_2 - u_1/y_3 - u_2$ has the nominal fuzzy model matrix as:

$$\bar{F}_{TS} = \begin{bmatrix} 0 & 0 & f_{TS,13} \\ f_{TS,21} & 0 & 0 \\ 0 & f_{TS,32} & 0 \end{bmatrix} \quad (4)$$

ii). Based on $\bar{F}_{TS}$, the control structure for the decentralized controller $G_C$ is determined by the principle that each non-zero element $f_{TS,ij}$ in $\bar{F}_{TS}$ is related to a sub-controller $g_{C,ji}$ which is in the transposed position [11]-[15]. Taking the system in (4) as an example, its decentralized controller is:

$$G_C = \begin{bmatrix} 0 & g_{C,12} & 0 \\ 0 & 0 & g_{C,23} \\ g_{C,31} & 0 & 0 \end{bmatrix} \quad (5)$$

iii). Based on $f_{TS,ij}$ s of the $n$ paired channels and the information provided by RNGA based criterion, $n$ ETSMs, denoted by $\hat{f}_{TS,ij}$s, can be constructed to represent the paired channels with coupling effects such that each non-zero element $g_{C,ij}$ in $G_C$ can be independently designed based on the $\hat{f}_{TS,ji}$. Taking (4) and (5) as an example, the decentralized control in Fig. 2(a) can be equivalently converted to three independent single control-loops in Fig. 2(b).

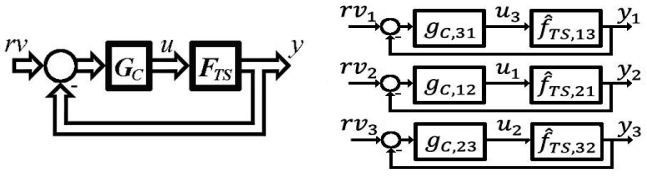


(a) (b)

Fig. 2. (a). a MIMO control-loop; (b). ETSM-based SISO control-loops

The ETSM based decentralized control strategy is a practical method that can be implemented without knowing the exact mathematical functions of the MIMO systems, and allows to directly apply the well-developed linear SISO control algorithms to regulate nonlinear multivariable systems. However, when there exists strong coupling effects among the paired channels, the decentralized control may not provide satisfactory performance due to the limited flexibility of its one-for-one control structure. In this paper, taking the decentralized control strategy in [15] as the basis, at first, improvements are made with respect to MIMO fuzzy modeling and ETSM

calculation. Afterwards, the sparse and decoupling control strategies that can improve the control system in terms of suppressing the coupling effects are developed.

## III. Fuzzy Modeling and Effective T-S Fuzzy Model Calculation for MIMO System

### A. Fuzzy modeling for MIMO systems

In the previous studies [3],[11],[15], each $f_{TS,ij}$ in $F_{TS}$ is independently identified based on the input-output data sampled from the isolated $y_i - u_j$. This manner may not work for some complex MIMO systems where the data of the isolated channels cannot be derived. On the other hand, the computational cost can become a problem especially for the large-scale systems since $n^2$ fuzzy models need to be identified for an $n \times n$ system. To overcome these limits, this paper uses a different manner to derive $F_{TS}$ that only constructs one MIMO T-S fuzzy model for the $n \times n$ system based on the input-output data sampled from the overall system instead of that from isolated channels.

For an $n \times n$ system in Fig. 1, collect the input-output data samples as $z(k) = [x(k)^T\ y(k+1)^T]^T \in \mathbb{R}^{4n}$, where $x(k) = [y(k)^T\ y(k-1)^T\ u(k-\tau)^T]^T = [y_1(k)\ \cdots\ y_n(k)\ y_1(k-1)\ \cdots\ y_n(k-1)\ u_1(k-\tau_1)\ \cdots\ u_n(k-\tau_n)]^T \in \mathbb{R}^{3n}$, $\tau_j \geq 0$ is the delays of $u_j$ to the outputs, $k = 1, \cdots, N_z$, $N_z$ is the number of data samples. Based on $z(k)$, a type-1/type-2 T-S fuzzy model, which is composed of the following "If-Then" fuzzy rules and maps the relationship between $x(k)$ and $y(k+1)$, can be built to describe the MIMO system:

$$\begin{aligned}
&\textit{Rule } l\text{: If } x(k) \text{ is } \mathcal{X}^l\text{, Then}\\
&y_1^l(k+1) = a_{1,1}^l y_1(k) + a_{1,2}^l y_1(k-1)\\
&\quad + b_{11}^l u_1(k-\tau_1) + b_{12}^l u_2(k-\tau_2) + \cdots + b_{1n}^l u_n(k-\tau_n)\\
&y_2^l(k+1) = a_{2,1}^l y_2(k) + a_{2,2}^l y_2(k-1)\\
&\quad + b_{21}^l u_1(k-\tau_1) + b_{22}^l u_2(k-\tau_2) + \cdots + b_{2n}^l u_n(k-\tau_n)\\
&\qquad\vdots\\
&y_n^l(k+1) = a_{n,1}^l y_n(k) + a_{n,2}^l y_n(k-1)\\
&\quad + b_{n1}^l u_1(k-\tau_1) + b_{n2}^l u_2(k-\tau_2) + \cdots + b_{nn}^l u_n(k-\tau_n)
\end{aligned} \tag{6}$$

where $l = 1, \cdots, L$, $L$ is the number of fuzzy rules; $\mathcal{X}^l$ is a type-1 or type-2 fuzzy set to characterize $x(k)$, the type of $\mathcal{X}^l$ determines the type of the fuzzy model; the local models of a fuzzy rule are a batch of multiple-input single-output linear polynomials, $a_{i,1}^l$, $a_{i,2}^l$ and $b_{ij}^l$ $(i, j = 1, \cdots, n)$ are coefficients; $y_i^l(k+1)$ is the $l$th local output of $y_i$. The total output $y_i(k+1)$, $i = 1, \cdots, n$, is expressed by:

$$\begin{aligned}
y_i(k+1) &= a_{i,1}(k) y_i(k) + a_{i,2}(k) y_i(k-1) + b_{i1}(k) u_1(k-\tau_1)\\
&\quad + b_{i2}(k) u_2(k-\tau_2) + \cdots + b_{in}(k) u_n(k-\tau_n)
\end{aligned} \tag{7}$$

where $a_{i,1}(k)$, $a_{i,2}(k)$ and $b_{ij}(k)$ $(i, j = 1, \cdots, n)$ are weighted sums of $a_{i,1}^l$, $a_{i,2}^l$ and $b_{ij}^l$ $(i, j = 1, \cdots, n)$ respectively, and the weights are the fuzzy membership grades of $x(k)$ in $\mathcal{X}^l$s. When $\mathcal{X}^l$s are type-1 fuzzy sets, the fuzzy membership grade of $x(k)$ in $\mathcal{X}^l$ is a crisp number denoted by $\mu^l(x(k))$, which satisfies $0 \leq \mu^l(x(k)) \leq 1$ and $\sum_{l=1}^{L} \mu^l(x(k)) = 1$, and is calculated by the following equation [3],[11],[15]:

$$\mu^l\big(x(k)\big) = \begin{cases} 1, & if\ \|x(k) - x_c^l\| = 0 \\ 0, & if\ {}^{v=1,\cdots,L}_{v\neq l} \forall \|x(k) - x_c^v\| = 0 \\ \dfrac{1}{\sum_{v=1}^{L} \frac{\|x(k)-x_c^l\|^2}{\|x(k)-x_c^v\|^2}}, & else \end{cases} \tag{8}$$

where $x_c^l \in \mathbb{R}^{3n}$, $l = 1, \cdots, L$ are centers of the fuzzy sets. Then the coefficients in (7) for a type-1 fuzzy model are:

$$\begin{cases} a_{i,p}(k) = \sum_{l=1}^{L} \mu^l(x(k)) a_{i,p}^l, & p = 1,2 \\ b_{ij}(k) = \sum_{l=1}^{L} \mu^l(x(k)) b_{ij}^l, & j = 1, \cdots, n \end{cases} \tag{9}$$

When $\mathcal{X}^l$s are type-2 fuzzy sets, the fuzzy membership grade of $x(k)$ in $\mathcal{X}^l$ is an interval denoted by $\tilde{\mu}^l(x(k)) = [\underline{\mu}^l(x(k)), \overline{\mu}^l(x(k))]$, where $\underline{\mu}^l(x(k))$ and $\overline{\mu}^l(x(k))$ are the lower and upper bounds respectively that satisfy $0 \leq \underline{\mu}^l(x(k)) \leq \overline{\mu}^l(x(k)) \leq 1$. In this paper, the bounds are calculated by:

$$\begin{cases} \underline{\mu}^l\big(x(k)\big) = \max\{0,\ \ \mu^l\big(x(k)\big) - \Delta\mu^l\} \\ \overline{\mu}^l\big(x(k)\big) = \min\{1,\ \ \mu^l\big(x(k)\big) + \Delta\mu^l\} \end{cases} \tag{10}$$

where $0 \leq \Delta\mu^l < 1$ denotes the varying range of the interval fuzzy membership grade $\tilde{\mu}^l(x(k))$ centered by $\mu^l(x(k))$. Then the coefficients in (7) for a type-2 fuzzy model are [11]:

$$\begin{cases} a_{i,p}(k) = \frac{1}{2}\left(\frac{\sum_{l=1}^{L} \underline{\mu}^l(x(k)) a_{i,p}^l}{\sum_{l=1}^{L} \underline{\mu}^l(x(k))} + \frac{\sum_{l=1}^{L} \overline{\mu}^l(x(k)) a_{i,p}^l}{\sum_{l=1}^{L} \overline{\mu}^l(x(k))}\right), & p = 1,2 \\ b_{ij}(k) = \frac{1}{2}\left(\frac{\sum_{l=1}^{L} \underline{\mu}^l(x(k)) b_{ij}^l}{\sum_{l=1}^{L} \underline{\mu}^l(x(k))} + \frac{\sum_{l=1}^{L} \overline{\mu}^l(x(k)) b_{ij}^l}{\sum_{l=1}^{L} \overline{\mu}^l(x(k))}\right), & j = 1, \cdots, n \end{cases} \tag{11}$$

The detailed steps to identify the type-1 and type-2 T-S fuzzy models can be found in [11],[15]. In order to make the development of sparse and decoupling control strategies more straightforward and understandable, we rewrite the $n$ total outputs in (7) in a form similar to the discrete transfer function matrix as follows:

$$\begin{aligned}
y(k) &= G(k, z^{-1}) \cdot u(k) = \left[g_{ij}(k, z^{-1})\right]_{n\times n} \cdot u(k)\\
&= \left[\frac{b_{ij}(k) z^{-(\tau_j+1)}}{1 - a_{i,1}(k) z^{-1} - a_{i,2}(k) z^{-2}}\right]_{n\times n} \cdot u(k)
\end{aligned} \tag{12}$$

where $z^{-1}$ is a backshift operator. From (12), we can know that $F_{TS} = F_{TS}(k, z^{-1}) = G(k, z^{-1})$ and $f_{TS,ij} = f_{TS,ij}(k, z^{-1}) = g_{ij}(k, z^{-1})$.

**Remark 2.1**: Compared to the fuzzy modeling in [3],[11],[15] that independently identifies each $f_{TS,ij}$ based on the data of isolated $y_i - u_j$, the manner developed in this paper is more practical and feasible since the input-output data of the overall system are more obtainable than that of the isolated channels. In addition, the time-varying coefficients $a_{i,1}(k)$, $a_{i,2}(k)$ and $b_{ij}(k)$ of all elements in $G(k, z^{-1})$ share the same fuzzy membership grades. Hence, the computational complexity and cost on both modeling and online calculation for the fuzzy model based control can be greatly reduced.

### B. Effective T-S fuzzy model calculation

Based on the matrix $G(k,z^{-1})$ in (12), at each sampling time, the $\mathcal{k}_{ij}$ and $e_{ij}$ of each $f_{TS,ij}$ can be calculated by [3]:

$$\begin{cases} \mathcal{k}_{ij}(k) = \frac{b_{ij}(k)}{1-a_{i,1}(k)-a_{i,2}(k)} \\ e_{ij}(k) = \frac{1+a_{i,2}(k)}{1-a_{i,1}(k)-a_{i,2}(k)} \cdot \Delta T + \tau_j \cdot \Delta T \end{cases} \tag{13}$$

Then the RGA and RNGA can be derived using (1) and (2), and the input-output pairs with minimum coupling effects can be selected according to the pairing rules. In order to achieve the desired performance, the sub-controller design needs to know and consider these "minimum coupling effects". ETSM is an effective tool to describe the coupling effects. In the decentralized control strategy [15], for each paired channel, an ETSM can be derived by merging the coupling information given from the interaction measure into the coefficients of its original fuzzy model. Afterwards, the $n$ ETSMs which are regarded as $n$ non-interacting SISO systems can be used to approximately represent the $n \times n$ MIMO system, and then the decentralized controller design can be equivalently transformed to multiple independent single-loop controller designs. Since the ETSM has same structure but different coefficients compared to its original T-S fuzzy model, according to (12), for a pair $y_i - u_j$, its ETSM $\hat{f}_{TS,ij}$ can be expressed as:

$$\hat{f}_{TS,ij}(k,z^{-1}) = \frac{\hat{b}_{ij}(k) z^{-(\hat{\tau}_{ij}(k)+1)}}{1-\hat{a}_{ij,1}(k)z^{-1}-\hat{a}_{ij,2}(k)z^{-2}} \tag{14}$$

where $\hat{a}_{ij,1}(k)$, $\hat{a}_{ij,2}(k)$, $\hat{b}_{ij}(k)$ and $\hat{\tau}_{ij}(k)$ are the revised coefficients. Similar as (13), the steady-state gain and normalized integrated error of $\hat{f}_{TS,ij}$, which are $\hat{\mathcal{k}}_{ij}$ and $\hat{e}_{ij}$, can be calculated by:

$$\begin{cases} \hat{\mathcal{k}}_{ij}(k) = \frac{\hat{b}_{ij}(k)}{1-\hat{a}_{ij,1}(k)-\hat{a}_{ij,2}(k)} \\ \hat{e}_{ij} = \frac{1+\hat{a}_{ij,2}(k)}{1-\hat{a}_{ij,1}(k)-\hat{a}_{ij,2}(k)} \cdot \Delta T + \hat{\tau}_{ij}(k) \cdot \Delta T \end{cases} \tag{15}$$

By considering (3), (13), and (15), we have the following equations to calculate the ETSM's coefficients in (14):

$$\begin{cases} \hat{b}_{ij}(k) = b_{ij}(k)/\lambda_{ij}(k) \\ \hat{a}_{ij,1}(k) = a_{i,1}(k) + \big(1-\gamma_{ij}(k)\big)a_{i,2}(k) - \gamma_{ij}(k) + 1 \\ \hat{a}_{ij,2}(k) = \gamma_{ij}(k)a_{i,2}(k) + \gamma_{ij}(k) - 1 \\ \hat{\tau}_{ij}(k) = \gamma_{ij}(k) \cdot \tau_j \end{cases} \tag{16}$$

Note that the values of $\gamma_{ij} = \phi_{ij}/\lambda_{ij}$ of the paired channels are positive according to the pairing rules of the RNGA based criterion, which can guarantee the causality that $\hat{\tau}_{ij} \geq 0$.

In addition, it is important for the closed-loop control system to possess the integrity [13]-[15], which means the control system should remain stable whether any sub-control loops are removed or kept. Therefore, $\hat{f}_{TS,ij}$ should reflect the "worse" condition between the original coefficients of $f_{TS,ij}$ and those revised by (16) to serve the controller design. It is a common sense that larger $|\hat{b}_{ij}|$ and $\hat{\tau}_{ij}$ imply a more challenging condition for the control system's stability. Thus, the values of $\lambda_{ij}$ and $\gamma_{ij}$ used in (16) to calculate $\hat{f}_{TS,ij}$ are determined by:

$$\begin{cases} \lambda_{ij} = \min\{1, \quad \lambda_{ij}\} \\ \gamma_{ij} = \max\{1, \quad \gamma_{ij}\} \end{cases} \tag{17}$$

**Remark 2.2**: For the ETSM calculation in [15], only $b_{ij}$ and $\tau_j$ of $f_{TS,ij}$ are revised to derive $\hat{f}_{TS,ij}$ through $\hat{b}_{ij} = b_{ij}/\lambda_{ij}$ and $\hat{\tau}_{ij} = \gamma_{ij} \cdot \tau_j$. In a well-paired system, $\lambda_{ij}$s and $\phi_{ij}$s of the paired elements are close to 1, and consequently $\gamma_{ij}$s ($\gamma_{ij} = \phi_{ij}/\lambda_{ij}$) of the paired elements are close to 1. In this case, according to (16), $\hat{a}_{ij,p}$ is approximately equal to $a_{i,p}$ ($p = 1,2$). Thus, it is acceptable to keep $a_{i,1}$s and $a_{i,2}$s unchanged in $\hat{f}_{TS,ij}$ for the decentralized controller design. However, for the sparse and decoupling control strategies presented in the next section where the ETSMs for unpaired elements need to be calculated, only revising $b_{ij}$ and $\tau_j$ cannot reflect the correct coupling effects since the $\gamma_{ij}$s of those unpaired elements may not be close to 1. In this paper, all the coefficients of $f_{TS,ij}$ are revised to derive a $\hat{f}_{TS,ij}$ by (16), which can offer a more accurate result to ensure that the desired performance can be achieved in decentralized, sparse and decoupling control.

## IV. Sparse And Decoupling Control Strategies

### A. Sparse control strategy

Compared to decentralized control, sparse control utilizes a richer control structure that is determined by a nominal fuzzy model $\bar{F}_{TS}$ adding several unpaired elements with relatively large dominance to the paired structure. Taking (4) and (5) as an example, suppose the unpaired channels $y_2 - u_3$ and $y_3 - u_3$ are added, then $\bar{F}_{TS}$ and $G_C$ for sparse control are:

$$\bar{F}_{TS} = \begin{bmatrix} 0 & 0 & f_{TS,13} \\ f_{TS,21} & 0 & f_{TS,23} \\ 0 & f_{TS,32} & f_{TS,33} \end{bmatrix}, G_C = \begin{bmatrix} 0 & g_{C,12} & 0 \\ 0 & 0 & g_{C,23} \\ g_{C,31} & g_{C,32} & g_{C,33} \end{bmatrix}$$

RNGA based interaction measure can be used to assess the relative dominance of the unpaired elements. Swapping the columns of an $n \times n$ $F_{TS}$ to place the paired elements in the diagonal positions if necessary, $\bar{F}_{TS}$ for sparse control becomes:

$$\bar{F}_{TS} = \left[\vartheta_{ij} \cdot f_{TS,ij}\right]_{n\times n} \tag{18}$$

where $\vartheta_{ii} = 1$ and $\vartheta_{ij} = \{0,1\}$ for $i \neq j$. In this study, four interaction indexes, $\mathcal{A}_{Row} = \left[\alpha_{Row,ij}\right]_{n\times n}$, $\mathcal{A}_{Col} = \left[\alpha_{Col,ij}\right]_{n\times n}$, $\mathcal{B}_{Row} = \left[\beta_{Row,ij}\right]_{n\times n}$ and $\mathcal{B}_{Col} = \left[\beta_{Col,ij}\right]_{n\times n}$ defined as follows, are used to determine the values of $\vartheta_{ij}$s:

$$\begin{cases} \alpha_{Row,ij} = \left|\lambda_{ij}/\lambda_{ii}\right| \\ \alpha_{Col,ij} = \left|\lambda_{ij}/\lambda_{jj}\right| \end{cases} \tag{19}$$

$$\begin{cases} \beta_{Row,ij} = \left|\phi_{ij}/\phi_{ii}\right| = \left(\left|\lambda_{ij}/\lambda_{ii}\right|\right) \cdot \left(\left|\gamma_{ij}/\gamma_{ii}\right|\right) \\ \beta_{Col,ij} = \left|\phi_{ij}/\phi_{jj}\right| = \left(\left|\lambda_{ij}/\lambda_{jj}\right|\right) \cdot \left(\left|\gamma_{ij}/\gamma_{jj}\right|\right) \end{cases} \tag{20}$$

$\alpha_{Row,ij}$ (or $\alpha_{Col,ij}$) and $\beta_{Row,ij}$ (or $\beta_{Col,ij}$) compare the degree of independence of the unpaired element $y_i - u_j$ with that of the paired element $y_i - u_i$ (or $y_j - u_j$) in terms of steady and dynamic properties. Equations (19) and (20) imply that when

$\alpha_{Row,ij}$, $\alpha_{Col,ij}$, $\beta_{Row,ij}$ and $\beta_{Col,ij}$ are close to 1, the degree of independence of $y_i - u_j$ is similar to that of the paired elements. Accordingly, it has a relatively large dominance and is likely to be included into $\bar{F}_{TS}$ for sparse control. Given $\varepsilon_\alpha$ and $\varepsilon_\beta$ satisfying $0 < \varepsilon_\alpha, \varepsilon_\beta \leq 1$, $\vartheta_{ij}$ is determined by:

$$\vartheta_{ij} = \begin{cases} 1, & \varepsilon_\alpha \leq \alpha_{Row,ij}, \alpha_{Col,ij} \leq 1/\varepsilon_\alpha, \\ & and\ \varepsilon_\beta \leq \beta_{Row,ij}, \beta_{Col,ij} \leq 1/\varepsilon_\beta \\ 0, & else \end{cases} \quad (21)$$

Note that small/large $\varepsilon_\alpha$ and $\varepsilon_\beta$ select a rich/simple sparse control structure. Empirically, the values of $\varepsilon_\alpha$ and $\varepsilon_\beta$ are chosen from [0,1, 0.3] [11].

**Remark 3.1**: in [14], only the value of $|\phi_{ij}|/|\phi_{ii}| = (|\lambda_{ij}|/|\lambda_{ii}|) \cdot (|\gamma_{ij}|/|\gamma_{ii}|)$ is used to assess the relative dominance. It states that $|\lambda_{ij}|/|\lambda_{ii}|$ and $|\gamma_{ij}|/|\gamma_{ii}|$ of a selected unpaired element should not be very large or very small, and consequently it uses a criterion that an unpaired element $y_i - u_j$ is qualified to be added to the sparse control structure when $|\phi_{ij}|/|\phi_{ii}|$ is a moderate value which is in [0.15, 8]. However, a moderate $|\phi_{ij}|/|\phi_{ii}|$ may contain a very large $|\lambda_{ij}|/|\lambda_{ii}|$ and a very small $|\gamma_{ij}|/|\gamma_{ii}|$, or a very small $|\lambda_{ij}|/|\lambda_{ii}|$ and a very large $|\gamma_{ij}|/|\gamma_{ii}|$, and then the selection criterion given in [14] can lead to incorrect results. While in [11], improvements are made that two indexes, $\alpha_{ij} = 0.5 \times (|\lambda_{ij}|/|\lambda_{ii}| + |\lambda_{ij}|/|\lambda_{jj}|)$ and $\beta_{ij} = 0.5 \times (|\phi_{ij}|/|\phi_{ii}| + |\phi_{ij}|/|\phi_{jj}|) = 0.5 \times [(|\lambda_{ij}| \cdot |\gamma_{ij}|)/(|\lambda_{ii}| \cdot |\gamma_{ii}|) + (|\lambda_{ij}| \cdot |\gamma_{ij}|)/(|\lambda_{jj}| \cdot |\gamma_{jj}|)]$ are used to select the unpaired elements which satisfies $\varepsilon_\alpha \leq \alpha_{ij} \leq 1/\varepsilon_\alpha$ and $\varepsilon_\beta \leq \beta_{ij} \leq 1/\varepsilon_\beta$. In this study, a further detailed selection criterion with four indexes as (19)-(20) is employed to guarantee that the selected $y_i - u_j$ possesses relatively large dominance in terms of both steady and dynamic properties when compared to the paired elements $y_i - u_i$ and $y_j - u_j$.

Using the nominal fuzzy model $\bar{F}_{TS}$ in (18) to represent the MIMO system for sparse controller design, for a closed-loop control system in Fig. 1, an ideal design is that the forward path satisfies the following equation:

$$\bar{F}_{TS}(z^{-1}) \cdot G_C(z^{-1}) = diag\left\{\frac{\Delta T}{1-z^{-1}}, \frac{\Delta T}{1-z^{-1}}, \cdots, \frac{\Delta T}{1-z^{-1}}\right\} \in \mathbb{R}^{n \times n} \quad (22)$$

Then the controller $G_C$ is obtained by:

$$G_C(z^{-1}) = \bar{F}_{TS}\,(z^{-1})^{-1} \cdot diag\left\{\frac{\Delta T}{1-z^{-1}}, \frac{\Delta T}{1-z^{-1}}, \cdots, \frac{\Delta T}{1-z^{-1}}\right\} \quad (23)$$

It is generally difficult to directly obtain $\bar{F}_{TS}\,(z^{-1})^{-1}$. In this study, we use an ETSM-based manner to solve this problem. According to the definition of the dynamic RGA (DRGA) [10],[14], we have the following equation:

$$DRGA = \left[D\lambda_{ij}(z^{-1})\right]_{n \times n} = \bar{F}_{TS}\,(z^{-1}) \otimes \hat{\bar{F}}^*_{TS}(z^{-1}) \quad (24)$$

where $D\lambda_{ij} = \vartheta_{ij} \cdot f_{TS,ij}/\hat{f}_{TS,ij}$, and $\hat{\bar{F}}^*_{TS}$ is defined as:

$$\hat{\bar{F}}^*_{TS}(z^{-1}) = \left[\vartheta_{ij}/\hat{f}_{TS,ij}\right]_{n \times n} \quad (25)$$

Similar to RGA in (1), DRGA can be calculated by [10],[14]:

$$DRGA = \bar{F}_{TS}\,(z^{-1}) \otimes \bar{F}_{TS}(z^{-1})^{-T} \quad (26)$$

Equations (24) and (26) reveal an important relationship:

$$\bar{F}_{TS}(z^{-1})^{-1} = \hat{\bar{F}}^*_{TS}(z^{-1})^T = \left[\vartheta_{ji}/\hat{f}_{TS,ji}\right]_{n \times n} \quad (27)$$

Submitting (27) to (23), we can have:

$$G_C(z^{-1}) = \hat{\bar{F}}^*_{TS}(z^{-1})^T \cdot diag\left\{\frac{\Delta T}{1-z^{-1}}, \frac{\Delta T}{1-z^{-1}}, \cdots, \frac{\Delta T}{1-z^{-1}}\right\} = \left[\frac{\vartheta_{ji} \cdot \Delta T}{\hat{f}_{TS,ji} \cdot (1-z^{-1})}\right]_{n \times n} \quad (28)$$

Therefore, the non-zero elements in $G_C$ are derived by:

$$g_{C,ij} = \frac{\Delta T}{\hat{f}_{TS,ji} \cdot (1-z^{-1})} \Rightarrow \hat{f}_{TS,ji} \cdot g_{C,ij} = \frac{\Delta T}{1-z^{-1}} \quad (29)$$

The term $\hat{f}_{TS,ji} \cdot g_{C,ij}$ in (29) can be regarded as the forward path of a closed-loop SISO control system as illustrated in Fig. 2(b), and the controller satisfying (29) is an ideal design for this single loop. By considering the delays, (29) is rewritten as

$$\hat{f}_{TS,ji}(k, z^{-1}) \cdot g_{C,ij}(k, z^{-1}) = \frac{z^{-\hat{\tau}_{ji}(k)} \cdot \Delta T}{1-z^{-1}} \quad (30)$$

Note that when all $\vartheta_{ij}$s ($i \neq j$) are 0, (29) tallies with the theory of ETSM-based decentralized control strategy in [15]. Therefore, both decentralized and sparse controllers can be realized by devising multiple independent single-loop controllers based on ETSMs. In order to maintain the integrity of the control system, $\hat{f}_{TS,ij}$s are calculated by (16) with $\lambda_{ij}$s and $\gamma_{ij}$s determined by (17).

Theoretically, any linear SISO control algorithms can be applied to design the sub-controllers based on their associated ETSMs. We leave the choice of linear SISO control algorithms to users. The stability of the sparse control strategy can be evaluated through the following procedure:

- The sparse controller can be expressed by:

$$\Delta u(k) = \bar{\mathfrak{K}}(k) \cdot \Delta \bar{X}(k) = \begin{bmatrix} \bar{\mathfrak{K}}_{11}(k) & \vartheta_{21}\bar{\mathfrak{K}}_{21}(k) & \cdots & \vartheta_{n1}\bar{\mathfrak{K}}_{n1}(k) \\ \vartheta_{12}\bar{\mathfrak{K}}_{12}(k) & \bar{\mathfrak{K}}_{22}(k) & \cdots & \vartheta_{n2}\bar{\mathfrak{K}}_{n2}(k) \\ \vdots & \vdots & \ddots & \vdots \\ \vartheta_{1n}\bar{\mathfrak{K}}_{1n}(k) & \vartheta_{2n}\bar{\mathfrak{K}}_{2n}(k) & \cdots & \bar{\mathfrak{K}}_{nn}(k) \end{bmatrix} \Delta \bar{X}(k) \quad (31)$$

  where $\Delta u(k) = u(k) - u(k-1)$ is the increment of the manipulated variable, $\Delta \bar{X}(k) = [\Delta \bar{X}_1(k)^T\ \Delta \bar{X}_2(k)^T\ \cdots\ \Delta \bar{X}_n(k)^T]^T$, $\Delta \bar{X}_i(k) = [d_i(k - m_i)\ \cdots\ d_i(k-1)\ d_i(k)]^T \in \mathbb{R}^{m_i+1}$, where $m_i$ ($i = 1, \cdots, n$) is a integer, $d_i(k) = rv_i(k) - y_i(k)$; $\bar{\mathfrak{K}}_{ij}(k) = [\bar{\mathfrak{K}}_{ij,m_i}(k)\ \bar{\mathfrak{K}}_{ij,m_i-1}(k)\ \cdots\ \bar{\mathfrak{K}}_{ij,1}(k)\ \bar{\mathfrak{K}}_{ij,0}(k)] \in \mathbb{R}^{1 \times (m_i+1)}$ consists of the control gains of $g_{C,ji}$ calculated based on $\hat{f}_{TS,ij}$ and $\Delta \bar{X}_i(k)$ using the selected linear control algorithm.
- The fuzzy model (7) or (12) for the MIMO system can be rewritten as:

$$\Delta \bar{X}(k+1) = \bar{A}(k)\Delta \bar{X}(k) + \bar{B}(k)\Delta u(k) \quad (32)$$

  where $\bar{A}(k) = diag\{\bar{A}_1(k), \cdots, \bar{A}_n(k)\}$, $\bar{A}_i(k) =$

$\begin{bmatrix} 0_{m_i\times 1} & I_{m_i\times m_i} \\ 0 & \bar{a}_i(k) \end{bmatrix} \in \mathbb{R}^{(m_i+1)\times(m_i+1)}$ , $\bar{a}_i(k) = [0\ \cdots 0\ a_{i,2}(k)\ a_{i,1}(k)] \in \mathbb{R}^{1\times m_i}$ ; $\bar{B}(k) = [\bar{B}_1(k)^T\ \cdots\ \bar{B}_n(k)^T]^T \in \mathbb{R}^{(n+\sum_{i=1}^{n} m_i)\times n}$, $\bar{B}_i(k) = \begin{bmatrix} 0_{m_i\times n} \\ \bar{b}_i(k) \end{bmatrix}$, $\bar{b}_i(k) = [b_{i1}(k)\ b_{i2}(k)\ \cdots\ b_{in}(k)] \in \mathbb{R}^{1\times n}$.

- Submitting (31) to (32), we can have:

$$\Delta\bar{X}(k+1) = \bar{A}(k)\Delta\bar{X}(k) + \bar{B}(k)\bar{\mathfrak{K}}(k)\Delta\bar{X}(k) = [\bar{A}(k) + \bar{B}(k)\bar{\mathfrak{K}}(k)]\Delta\bar{X}(k) \quad (33)$$

The control-loop using the proposed sparse control strategy is stable if all the eigenvalues of $\bar{A}(k) + \bar{B}(k)\bar{\mathfrak{K}}(k)$ lie inside the unit cycle.

### B. *Decoupling control strategy*

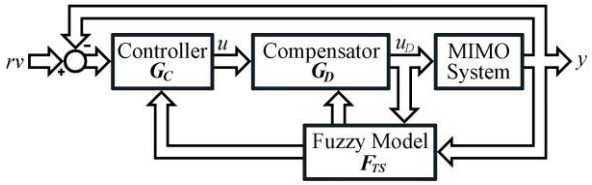


Fig. 3. Fuzzy model based decoupling control system

Decoupling control strategy is to insert a decoupling compensator between the decentralized controller and the MIMO system in order to compensate for the coupling effects among the pairs. In Fig. 3, $G_D = \left[g_{D,ij}\right]_{n\times n}$ denotes the fuzzy model based decoupling compensator, and $u_D \in \mathbb{R}^n$ is the output of $G_D$. Suppose the paired elements are placed in the diagonal positions, a perfect decoupling compensator can eliminate all the off-diagonal elements and only leave the diagonal elements for decentralized controller design. Using $F_{TS}(z^{-1})$ to represent the MIMO system, the compensator $G_D(z^{-1})$ is required to satisfy:

$$F_{TS,D}(z^{-1}) = F_{TS}(z^{-1})\cdot G_D(z^{-1}) = diag\left\{f_{TS,11}^{(0)} z^{-T_1}, f_{TS,22}^{(0)} z^{-T_2}, \cdots, f_{TS,nn}^{(0)} z^{-T_n}\right\} \quad (34)$$

where $F_{TS,D}$ denotes the decoupled MIMO fuzzy model, in which $f_{TS,jj}^{(0)}(k,z^{-1}) = \frac{b_{jj}(k)z^{-1}}{1-a_{j,1}(k)z^{-1}-a_{j,2}(k)z^{-2}}$ is equal to the $f_{TS,jj}(k,z^{-1})$ in (12) with $z^{-\tau_j}$ removed, and $z^{-T_j}$, $j = 1,\cdots,n$, is the delay used to guarantee the causality of $G_D(z^{-1})$. According to (34), $G_D(z^{-1})$ is derived by:

$$G_D(z^{-1}) = F_{TS}(z^{-1})^{-1}\cdot F_{TS,D}(z^{-1}) \quad (35)$$

In (35), $F_{TS}(z^{-1})^{-1}$ is generally difficult to derive. Inspired by (27), ETSMs can be employed to solve this problem:

$$F_{TS}(z^{-1})^{-1} = \hat{F}_{TS}^{*}(z^{-1})^T = \left[1/\hat{f}_{TS,ji}\right]_{n\times n} \quad (36)$$

Submitting (36) to (35), $G_D(z^{-1})$ can be derived by:

$$G_D(z^{-1}) = \hat{F}_{TS}^{*}(z^{-1})^T\cdot F_{TS,D}(z^{-1}) = \left[\frac{f_{TS,jj}^{(0)} z^{-T_j}}{\hat{f}_{TS,ji}}\right]_{n\times n} \quad (37)$$

By submitting (12) and (14) into (37), the decoupling compensator can be further expressed as:

$$G_D(k,z^{-1}) = \left[g_{D,ij}(k,z^{-1})\right]_{n\times n} = \left[\frac{(1-\hat{a}_{ji,1}(k)z^{-1}-\hat{a}_{ji,2}(k)z^{-2})b_{jj}(k)}{(1-a_{j,1}(k)z^{-1}-a_{j,2}(k)z^{-2})\hat{b}_{ji}(k)} z^{-(T_j(k)-\hat{\tau}_{ji}(k))}\right]_{n\times n} \quad (38)$$

Note that in (38), the coefficients of $\hat{f}_{TS,ij}$s calculated by (16) use the original values of $\lambda_{ij}$ and $\gamma_{ij}$ derived from (3) rather than the revised ones in (17) since it is used to obtain a decoupling compensator instead of being a virtual model reflecting the "worse" condition for controller design.

Compared with (27), equation (36) contains no $\vartheta_{ij}$s and leaves no "blank" for its elements. Hence, according to (34)-(38), $G_D$ in (38) uses a full-dimensional structure that can compensate for the coupling effects caused by all unpaired elements. To ensure $G_D$ to be physically realizable, the analysis is presented as follows:

- *Stability*: the elements of $G_D$ in (38) have the denominators same as that in the original fuzzy model $F_{TS}$ in (12), which implies $G_D$ is a stable system.
- *Properness*: each element of $G_D$ satisfies that the numerator's degree does not exceed the denominator's. In order to guarantee the properness of the decoupling compensator that each element satisfies $\lim_{z\to\infty}\left|g_{D,ij}(k,z^{-1})\right| < \infty$, for the $g_{D,ij}$, when the $\hat{b}_{ji}(k) = 0$ $(i,j = 1,\cdots,n)$, let it be a small value close to 0, such as let $\hat{b}_{ji}(k) = 10^{-6}$.
- *Causality*: in order to guarantee $G_D$ to be a casual system, the delays $z^{-T_j(k)}$ $(j = 1,\cdots,n)$ in (38) are determined by:

$$T_j(k) = \max\left\{\hat{\tau}_{j1}(k), \hat{\tau}_{j2}(k), \cdots, \hat{\tau}_{jn}(k)\right\}$$

With the decoupling compensator in (38) inserted into the control-loop, in theory, each non-zero element of the decentralized controller $G_C$ can be independently design based on a SISO T-S fuzzy model $f_{TS,jj}^{(0)} z^{-T_j}$ using suitable linear control algorithms. The choice of SISO linear control algorithm is determined by users. The stability of the decoupling control strategy can be evaluated through the following procedure:

- The controller (decentralized) can be expressed by:

$$\Delta\mathbf{u}(k) = \bar{\mathfrak{K}}(k)\Delta\bar{\mathfrak{X}}(k) \quad (39)$$

where $\Delta\mathbf{u}(k) = [\Delta u(k-2)^T\ \Delta u(k-1)^T\ \Delta u(k)^T]^T$, $\Delta\bar{\mathfrak{X}}(k) = [\Delta\bar{X}(k-2)^T\ \Delta\bar{X}(k-1)^T\ \Delta\bar{X}(k)^T]^T$, and $\bar{\mathfrak{K}}(k) = diag\{\bar{\mathfrak{K}}(k-2), \bar{\mathfrak{K}}(k-1), \bar{\mathfrak{K}}(k)\} \in \mathbb{R}^{3n\times 3(n+\sum_{i=1}^{n} m_i)}$, the $\Delta u(k)$, $\Delta\bar{X}(k)$ and $\bar{\mathfrak{K}}(k)$ are same as that in (31) with all $\vartheta_{ij}$s $(i \neq j)$ are 0 because it is a decentralized controller.

- The decoupling compensator in (38) can be rewritten as:

$$\Delta\bar{u}_D(k+1) = A_D(k)\Delta\bar{u}_D(k) + B_D(k)\Delta\mathbf{u}(k)$$
$$\Delta u_D(k) = C_D\Delta\bar{u}_D(k) \quad (40)$$

where $\Delta\bar{u}_D(k) = [\Delta\bar{u}_{D,1}(k)^T\ \Delta\bar{u}_{D,2}(k)^T\cdots\Delta\bar{u}_{D,n}(k)^T]^T \in \mathbb{R}^{2n^2}$, $\Delta\bar{u}_{D,i}(k) = [\Delta\bar{u}_{D,i,1}(k-1)\ \Delta\bar{u}_{D,i,1}(k)\ \Delta\bar{u}_{D,i,2}(k-1)\ \Delta\bar{u}_{D,i,2}(k)\ \cdots\ \Delta\bar{u}_{D,i,n}(k-1)\ \Delta\bar{u}_{D,i,n}(k)]^T \in \mathbb{R}^{2n}$, $\Delta\bar{u}_{D,i,j}(k)$ is the incremental output of the element in row $i$ and column $j$ of the matrix $G_D(k,z^{-1})$ in (38); $A_D(k) = diag\{A_{D,1}(k),\cdots,A_{D,n}(k)\} \in \mathbb{R}^{2n^2\times 2n^2}$, where $A_{D,i}(k) =$

$diag\{A_{D,i,1}(k),\cdots,A_{D,i,n}(k)\}$, and in which $A_{D,i,j}(k) = \begin{bmatrix} 0 & 1 \\ a_{j,2}(k) & a_{j,1}(k) \end{bmatrix}$; $B_D(k) = [B_{D,1}(k)^T \cdots B_{D,n}(k)^T]^T\} \in \mathbb{R}^{2n^2\times 3n}$, where $B_{D,i}(k) = [B_{D,i,1}(k)^T \cdots B_{D,i,n}(k)^T]^T$, and $B_{D,i,j}(k) = \begin{bmatrix} 0_{1\times 3n} \\ -\frac{\hat{b}_{jj}(k)\hat{a}_{ji,2}(k)}{\hat{b}_{ji}(k)} I_j^T \quad -\frac{\hat{b}_{jj}(k)\hat{a}_{ji,1}(k)}{\hat{b}_{ji}(k)} I_j^T \quad \frac{\hat{b}_{jj}(k)}{\hat{b}_{ji}(k)} I_j^T \end{bmatrix}$, in which $I_j \in \mathbb{R}^n$ is a vector where the $j$th element is 1 and others are 0; $C_D = diag\{C_{D,1},\cdots,C_{D,n}\} \in \mathbb{R}^{n\times 2n^2}$, $C_{D,i} = [C_{D,i,1} \cdots C_{D,i,n}]$, and $C_{D,i,j} = [0 \quad 1]$, $i,j = 1,\cdots,n$.

- The fuzzy model (7) or (12) for the MIMO system can be rewritten as:

$$\Delta\bar{\mathfrak{X}}(k+1) = \bar{\mathfrak{A}}(k)\Delta\bar{\mathfrak{X}}(k) + \bar{\mathfrak{B}}(k)\Delta u_D(k) \tag{41}$$

where $\bar{\mathfrak{A}}(k) = diag\{\bar{A}(k-2),\bar{A}(k-1),\bar{A}(k)\}$, and $\bar{\mathfrak{B}}(k) = [\bar{B}(k-2)^T\ \bar{B}(k-1)^T\ \bar{B}(k)^T]^T$, the $\bar{A}(k)$ and $\bar{B}(k)$ are same as that in (32).

- The decoupling compensator (40) and the MIMO system (41) are connected in series, they constitute an augmented system expressed as:

$$\begin{bmatrix} \Delta\bar{u}_D(k+1) \\ \Delta\bar{\mathfrak{X}}(k+1) \end{bmatrix} = \begin{bmatrix} A_D(k) & 0_{2n^2\times 3(n+\sum_{i=1}^n m_i)} \\ \bar{\mathfrak{B}}(k)C_D & \bar{\mathfrak{A}}(k) \end{bmatrix} \begin{bmatrix} \Delta\bar{u}_D(k) \\ \Delta\bar{\mathfrak{X}}(k) \end{bmatrix} + \begin{bmatrix} B_D(k) \\ 0_{3(n+\sum_{i=1}^n m_i)\times 3n} \end{bmatrix} \Delta\mathbf{u}(k) \tag{42}$$

The equation (39) can be revised as:

$$\Delta\mathbf{u}(k) = [0_{3n\times 2n^2} \quad \bar{\mathfrak{K}}(k)] \begin{bmatrix} \Delta\bar{u}_D(k) \\ \Delta\bar{\mathfrak{X}}(k) \end{bmatrix} \tag{43}$$

- Submitting (43) to (42), we have

$$\begin{bmatrix} \Delta\bar{u}_D(k+1) \\ \Delta\bar{\mathfrak{X}}(k+1) \end{bmatrix} = \begin{bmatrix} A_D(k) & B_D(k)\bar{\mathfrak{K}}(k) \\ \bar{\mathfrak{B}}(k)C_D & \bar{\mathfrak{A}}(k) \end{bmatrix} \begin{bmatrix} \Delta\bar{u}_D(k) \\ \Delta\bar{\mathfrak{X}}(k) \end{bmatrix} \tag{44}$$

The decoupling control-loop can be considered to be stable if all the eigenvalues of $\begin{bmatrix} A_D(k) & B_D(k)\bar{\mathfrak{K}}(k) \\ \bar{\mathfrak{B}}(k)C_D & \bar{\mathfrak{A}}(k) \end{bmatrix}$ lie inside the unit cycle.

### C. Discussion

This section presents a sparse control strategy and a decoupling control strategy to enhance the capability of the decentralized control strategy in [15] with respect to suppressing the strong coupling effects among the paired channels in a MIMO system. The main contribution of this paper is that it develops the frameworks where conventional linear SISO control algorithms can be directly used to design controllers for the non-linear MIMO systems with closely coupled channels and without knowing accurate mathematical functions.

Sparse control is an intermediate between decentralized and centralized control. Compared to decentralized control, sparse control has more sub-controllers $g_{C,ij}$s in $G_C$ and thus provides increased design degree of freedom to handle the coupling effects. While compared to centralized control, sparse control is "economical" that leaves the sub-controllers related to the non-significant channels to be blank in $G_C$, and uses the sub-controllers related to the dominant channels to conquer all the interactions.

Decoupling control employs a decoupling compensator to offset the coupling effects caused by the unpaired elements, and then the paired channels are decoupled to the extent that the MIMO system can be regarded as multiple non-interacting SISO systems to facilitate decentralized controller design. The decoupling compensator in (38) avoids the complex calculations to derive the inverse of the MIMO system dynamics, and can be easily realized in real applications since its elements have very simple structures and the coefficients are easy to compute.

The indexes proposed in (19) and (20) to select sparse control structure need to properly predefine a $\varepsilon_\alpha$ and a $\varepsilon_\beta$ which have marked impacts on the sparse control performance, and the sparse control requires a control algorithm to have a certain degree of margin to be tolerant for the coupling effects from the unselected elements. While the decoupling control strategy does not require any predefined coefficients for control structure selection, and its controller design is not required to reach the level of robustness as that of the sparse control since the decoupling compensator is a qualified assistant to clean the coupling effects. In theory, the decoupling control using a full-dimensional compensator can achieve better performance than the sparse control. However, the cost to achieve this full-dimensional compensator may be higher than that of the sparse control strategy, especially for large-scale MIMO systems and when the sparse control structure is "sparse" and the algorithms to design and tune the sub-controllers are computationally inexpensive. In addition, one thing needs to be noted that the delays of the output responses under the sparse control will not exceed those under the decoupling control.

According to the characteristics of the two proposed control strategies, in the case that when decentralized control cannot fully handle the channel interactions, if a small part of the unpaired elements has the relatively large dominance, the sparse control strategy can be applied to improve the performance instead of using the full-dimensional decoupling compensator. If a large part of the unpaired elements is selected, which means a "dense" instead of a "sparse" control structure is required for regulating the MIMO system, it will be better to employ the decoupling control strategy to save the cost in design and tuning for the sub-controllers.

## V. Case Studies

### A. Example-I

Consider the following nonlinear 3 × 3 system from [15]:

$$\begin{aligned}
\dot{\mathbb{x}}_1 &= \mathbb{x}_2 + 5\mathbb{x}_1^2\mathbb{x}_2 + 6\mathbb{x}_2^2 \\
\dot{\mathbb{x}}_2 &= -4\mathbb{x}_1 - 5\mathbb{x}_2 + 8\mathbb{x}_1\mathbb{x}_2 + u_1 \\
\dot{\mathbb{x}}_3 &= \mathbb{x}_4 \\
\dot{\mathbb{x}}_4 &= -6\mathbb{x}_3 - 5\mathbb{x}_4 + 3\mathbb{x}_3^3 + 10\mathbb{x}_3\mathbb{x}_4\mathbb{x}_5 + u_2 \\
\dot{\mathbb{x}}_5 &= \mathbb{x}_6 + 4\mathbb{x}_7^2 \\
\dot{\mathbb{x}}_6 &= \mathbb{x}_7 + 5\mathbb{x}_5\mathbb{x}_6^2\mathbb{x}_7 \\
\dot{\mathbb{x}}_7 &= -14\mathbb{x}_5 - 23\mathbb{x}_6 - 10\mathbb{x}_7 + 7\mathbb{x}_5\mathbb{x}_6\mathbb{x}_7 + u_3 \\
y_1 &= 5\mathbb{x}_1 + 5\mathbb{x}_2 + 6\mathbb{x}_3 + 2\mathbb{x}_4 + 14\mathbb{x}_5 + 9\mathbb{x}_6 + \mathbb{x}_7
\end{aligned}$$

$$y_2 = 8\mathbb{x}_1 + 2\mathbb{x}_2 + 3\mathbb{x}_3 + 4\mathbb{x}_5 + 6\mathbb{x}_6 + 2\mathbb{x}_7$$
$$y_3 = \mathbb{x}_1 + \mathbb{x}_2 + 4\mathbb{x}_3 + 2\mathbb{x}_4 + 1.4\mathbb{x}_5 + 0.2\mathbb{x}_6 \quad (45)$$

where $\mathbb{x}_r$s $(r = 1, \cdots, 7)$ are states. Suppose the mathematical function of the system in (45) is unknown to the controller designer, and there exists noise in the sampled inputs random but bounded in $[-0.1,\ 0.1]$. The sampling time is $\Delta T = 0.1s$, and the delays are $\tau_{i1} = \tau_{i2} = 20$ and $\tau_{i3} = 10$, $i = 1,2,3$. Given the number of fuzzy rules as $L = 6$, the type-1 and type-2 T-S fuzzy models with the structure in (6) can be identified based on the input-output data using the method introduced in [11]. Due to the limited space, we only present the first rule:

*Rule* 1: If $x(k)$ is $\mathcal{X}^1$, Then
$y_1^1(k+1) = 1.1546y_1(k) - 0.3536y_1(k-1)$
$+0.2684u_1(k-20) + 0.2012u_2(k-20) + 0.2233u_3(k-10)$
$y_2^1(k+1) = 1.3306y_2(k) - 0.4080y_2(k-1)$
$+0.1578u_1(k-20) + 0.0343u_2(k-20) + 0.0213u_3(k-10)$
$y_3^1(k+1) = 1.0136y_3(k) - 0.2437y_3(k-1)$
$+0.0616u_1(k-20) + 0.1554u_2(k-20) + 0.0284u_3(k-10)$

where the center of $\mathcal{X}^1$ is $x_c^1 = [1.2601\ \ 1.8746\ \ 0.2419\ \ 1.2593\ \ 1.8536\ \ 0.2411\ \ 1.0000\ \ -0.0245\ \ -0.0504]^T$, and $\Delta\mu^1 = 0.5057$ for the first type-2 fuzzy set. The comparisons between real outputs and fuzzy models' outputs with the root-mean-square-errors (RMSEs) are shown in Fig. 4. The type-2 fuzzy model achieves higher accuracy when compared to its type-1 counterpart.

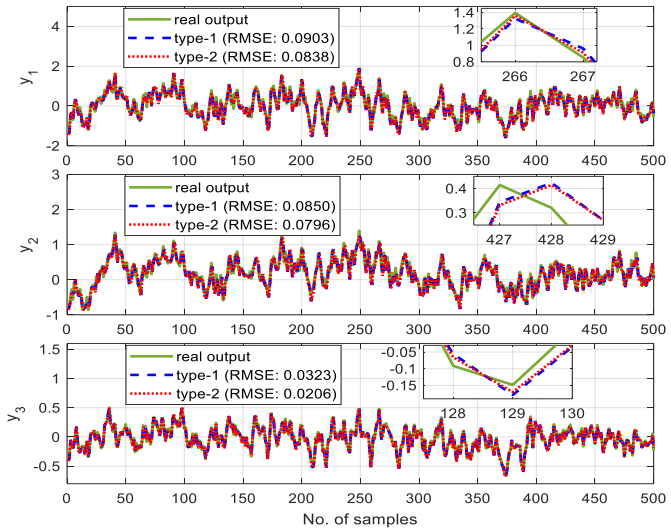


Fig. 4. Comparisons of real outputs and fuzzy models' outputs for (45)

The elements in $\mathcal{K} = [\mathcal{k}_{ij}]_{n\times n}$, $\mathcal{E} = [e_{ij}]_{n\times n}$, RGA and RNGA calculated from the fuzzy models are time-varying. Using the results derived from the type-2 T-S fuzzy model and calculated at the operating point $x(k) = [0\ \cdots 0]^T \in \mathbb{R}^9$ as an example, the matrices are:

$$\mathcal{K} = \begin{bmatrix} 1.2784 & 0.9791 & 0.9808 \\ 1.8811 & 0.4818 & 0.2734 \\ 0.2563 & 0.6742 & 0.0839 \end{bmatrix}, \mathcal{E} = \begin{bmatrix} 2.4464 & 2.4464 & 1.4464 \\ 3.0917 & 3.0917 & 2.0917 \\ 2.3912 & 2.3912 & 1.3912 \end{bmatrix}$$

$$RGA = \begin{bmatrix} -0.2157 & -0.1006 & 1.3164 \\ 1.2773 & -0.0814 & -0.1959 \\ -0.0616 & 1.1821 & -0.1205 \end{bmatrix}$$

$$RNGA = \begin{bmatrix} -0.1759 & -0.1112 & 1.2871 \\ 1.2460 & -0.0787 & -0.1673 \\ -0.0701 & 1.1898 & -0.1197 \end{bmatrix}$$

The pairing structure determined by the above RGA and RNGA is $y_1 - u_3/y_2 - u_1/y_3 - u_2$, which is same to that in [15]. From the RGA and RNGA, we have:

$$\mathcal{A}_{Row} = \begin{bmatrix} 0.1639 & 0.0764 & 1 \\ 1 & 0.0638 & 0.1533 \\ 0.0521 & 1 & 0.1019 \end{bmatrix}, \mathcal{A}_{Col} = \begin{bmatrix} 0.1689 & 0.0851 & 1 \\ 1 & 0.0689 & 0.1488 \\ 0.0482 & 1 & 0.0915 \end{bmatrix}$$

$$\mathcal{B}_{Row} = \begin{bmatrix} 0.1367 & 0.0864 & 1 \\ 1 & 0.0631 & 0.1343 \\ 0.0589 & 1 & 0.1006 \end{bmatrix}, \mathcal{B}_{Col} = \begin{bmatrix} 0.1412 & 0.0934 & 1 \\ 1 & 0.0661 & 0.1300 \\ 0.0563 & 1 & 0.0930 \end{bmatrix}$$

Choosing $\varepsilon_\alpha = \varepsilon_\beta = 0.1$, the selected unpaired elements for sparse control are $y_1 - u_1$ and $y_2 - u_3$. Note that the results calculated from the type-1 fuzzy model give the same pairing structure and select same unpaired elements. During the whole control period, the pairing structure and sparse control structure for this MIMO system remain unchanged.

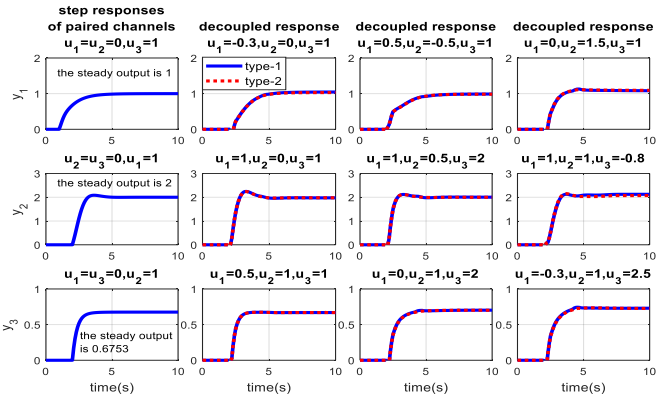


Fig. 5. The step responses of the three paired channels of (45)

A decoupling compensator is calculated using (38) for this MIMO system. In order to exhibit its performance, the comparisons of the step responses of isolated paired channels (for example, for the pair $y_1 - u_3$, set $u_3 = 1$ and $u_1 = u_2 = 0$ to have the step response of isolated $y_1 - u_3$) and the decoupled responses (for instance, for the pair $y_1 - u_3$, keep $u_3 = 1$ and randomly choose the values for the other two inputs) are shown in Fig. 5. From Fig. 5, for each pair, when other two inputs are with different values, the changes in its step response are very small, which demonstrates that the compensator can reduce the coupling effects to a great extent.

The ETSM-based decentralized, sparse and decoupling controllers can all be realized by designing multiple independent single control-loops. The gain and phase margins based SISO control algorithm used in [15] is selected to design each sub-controllers with the gain and phase margins set as 3 and $\pi/3$, respectively. Given the references as $rv_1 = 0.3$, $rv_2 = 1$ and $rv_3 = 0$, the performances of the three control strategies, as well as the type-2 fuzzy model based decentralized control of [15] are shown in Fig. 6. Besides, the integrated absolute errors (IAEs) of these control performances are presented in Table 1. The decentralized control of [15] gives the longest settling time for three outputs, and the decentralized control in this paper gives largest overshoots in $y_1$ and $y_3$, the performance of the decentralized control in this paper is better than that of [15] for $y_2$. The outputs under the sparse control go to the direction opposite to the references at the beginning, and return to the right direction after a while, thus they have large IAEs. The decoupling control achieves the minimum values in overshoots and settling time as well as IAEs among the three

control strategies. Note that the control performances can be improved by further tuning the gain and phase margins, or using a different SISO control algorithm. From Fig. 6 and Table 1, type-1 and type-2 fuzzy models have comparable performance.

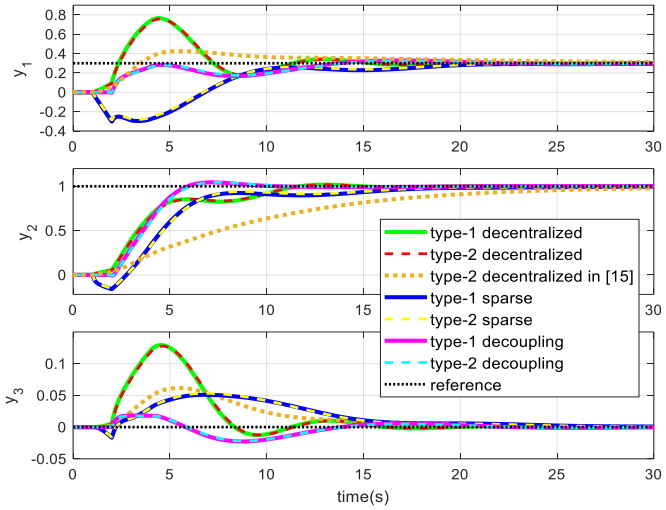


Fig. 6. Comparisons of different control strategies for the original system (45)

Table 1. The IAEs of the control performances in Fig. 6

| Controllers | $y_1$ | $y_2$ | $y_3$ |
|---|---|---|---|
| Type-1 decentralized | 1.9902 | 5.7633 | 0.6571 |
| Type-2 decentralized | 1.9827 | 5.7302 | 0.6569 |
| Type-2 decentralized [15] | 2.2155 | 9.6638 | 0.4615 |
| Type-1 sparse | 5.7565 | 8.0116 | 0.6693 |
| Type-2 sparse | 5.5517 | 7.8596 | 0.6683 |
| Type-1 decoupling | 1.7491 | 3.9753 | 0.1982 |
| Type-2 decoupling | 1.7262 | 3.9222 | 0.1903 |

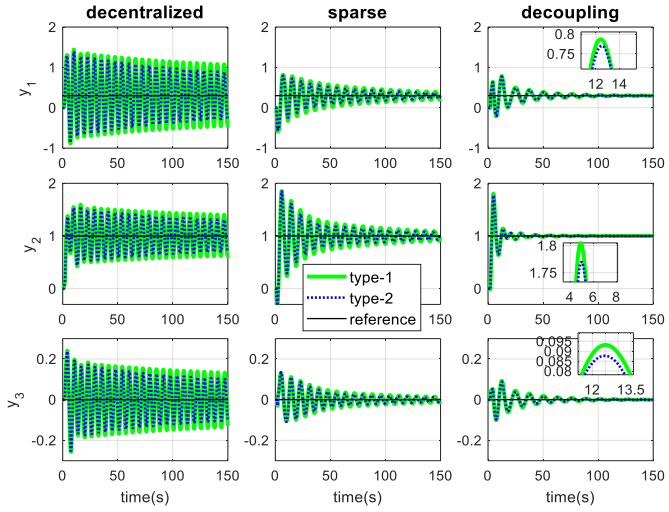


Fig. 7. Comparisons of three control strategies for Case-I of (45)

In order to test the robustness of the three control strategies, we suppose the gains of the system inputs in (45), which originally are 1, are enlarged to the following two cases due to the uncertainties:

**Case-I**: the gains of inputs become 2.7

**Case-II**: the gains of inputs become 3

The controllers designed for the original system are used to manipulate the revised systems of Case-I and Case-II. The results are shown in Figs. 7 and 8. From Fig. 7 for Case-I, the decentralized control leads to oscillations in the responses, and the outputs under the sparse control can finally reach their references after a period of time. The decoupling control offers the best performance among the three control strategies in terms of overshoot and settling time. The IAEs in Table 2 also demonstrate this fact. From Fig. 8 for Case-II where the uncertainty is further enlarged, the system becomes divergent under the decentralized control, and is oscillating under the sparse control. While under the decoupling control, the outputs of the system can stably reach their references. In both Case-I and Case-II, type-2 fuzzy model outperforms its type-1 counterpart with respect to overshoot, oscillating amplitude and IAE, which is more apparent under larger uncertainties.

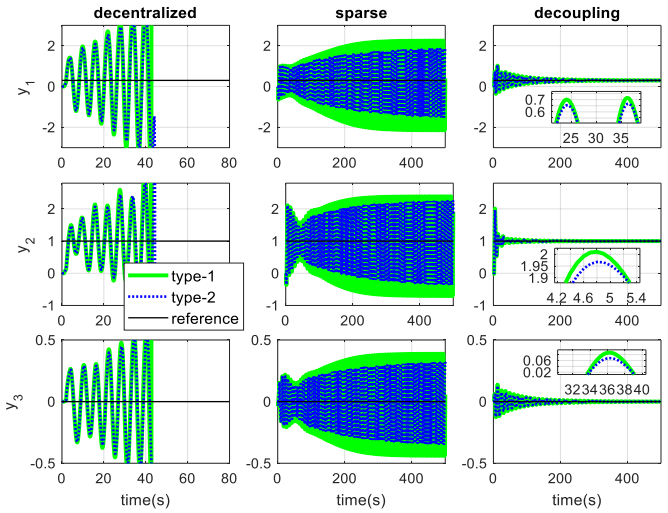


Fig. 8. Comparisons of three control strategies for Case-II of (45)

Table 2. The IAEs of the control performances in Figs. 7 and 8

| Cases | Controllers | $y_1$ | $y_2$ | $y_3$ |
|---|---|---|---|---|
| Case-I | Type-1 sparse | 31.5770 | 33.5127 | 5.0966 |
| | Type-2 sparse | 25.0187 | 27.5825 | 4.3525 |
| | Type-1 decoupling | 10.2197 | 7.1979 | 1.9773 |
| | Type-2 decoupling | 9.5811 | 6.9971 | 1.7333 |
| Case-II | Type-1 decoupling | 33.6333 | 12.3352 | 6.8939 |
| | Type-2 decoupling | 30.9843 | 11.5228 | 5.7087 |

The results in Figs. 7 and 8 demonstrate that sparse control with extra sub-controllers is more robust than its decentralized counterpart, and decoupling control outperforms both decentralized and sparse counterparts, especially when the uncertainties are enlarged and strong coupling effects appear, which validates the discussion in Section III.

### *B. Example-II*

Consider a system of two continuous stirred-tank reactor [35] as shown in Fig. 9, where $F_*$, $T_*$, $C_*$, and $V_*/V$ denote flow rate, temperature, concentration, and volume, respectively. $T_{j10}$, $T_{j20}$, and $C_{A0}$ are used to regulate $T_1$, $T_2$, and $C_{A2}$. This system can be expressed by the following six nonlinear ordinary differential equations with the parameters given in Table 3:

$$\dot{\mathbb{x}}_{11} = (T_1^d - \mathbb{x}_{11} + \mathbb{x}_{31} + T_2^d)(F + F_R)/V - (\mathbb{x}_{11} + \mathbb{x}_{12} + T_2^d - T_{j2}^d)UA/(\rho c_p V) - \left(C_{A2}^d + \mathbb{x}_{21}\right)e^{-E/R\left(\mathbb{x}_{11}+T_2^d\right)}\theta\delta/(\rho c_p)$$

$$\dot{\mathbb{x}}_{12} = \left(\mathbb{x}_{11} + T_2^d - \mathbb{x}_{12} - T_{j2}^d\right)UA/(\rho_j c_j V_j) + \left(u_1 + T_{j20}^d - \mathbb{x}_{12} - T_{j2}^d\right)F_{j2}/V_j$$

$$\dot{\mathbb{x}}_{21} = \left(C_{A1}^d + \mathbb{x}_{22}\right)(F + F_R)/V - \left((F + F_R)/V + \theta e^{-E/R\left(\mathbb{x}_{11}+T_2^d\right)}\right)\left(\mathbb{x}_{21} + C_{A2}^d\right)$$

$$\dot{\mathbb{x}}_{22} = \left(C_{A2}^d + \mathbb{x}_{21}\right)F_R/V - \left((F+F_R)/V + \theta e^{-E/R\left(\mathbb{x}_{31}+T_1^d\right)}\right)\left(\mathbb{x}_{22} + C_{A1}^d\right) + \left(u_2 + C_{A0}^d\right)F_0/V$$
$$\dot{\mathbb{x}}_{31} = \left(T_2^d + \mathbb{x}_{11}\right)F_R/V - \left(\mathbb{x}_{31} + T_1^d\right)(F+F_R)/V - e^{-E/R\left(\mathbb{x}_{31}+T_1^d\right)}\left(\mathbb{x}_{22} + C_{A1}^d\right)\theta\delta/(\rho c_p) - \left(\mathbb{x}_{31} + \mathbb{x}_{32} + T_1^d - T_{j1}^d\right)UA/(\rho c_p V) + T_0^d F_0/V$$
$$\dot{\mathbb{x}}_{32} = \left(\mathbb{x}_{31} - \mathbb{x}_{32} + T_1^d - T_{j1}^d\right)UA/(\rho_j c_j V_j) + \left(u_3 + T_{j10}^d - \mathbb{x}_{32} - T_{j1}^d\right)F_{j1}/V_j \quad (46)$$

where $\mathbb{x}_{11} = T_2 - T_2^d$, $\mathbb{x}_{12} = T_{j2} - T_{j2}^d$, $\mathbb{x}_{21} = C_{A2} - C_{A2}^d$, $\mathbb{x}_{22} = C_{A1} - C_{A1}^d$, $\mathbb{x}_{31} = T_1 - T_1^d$ and $\mathbb{x}_{32} = T_{j1} - T_{j1}^d$. A MIMO system can be formed with three inputs: $u_1 = T_{j20} - T_{j20}^d$, $u_2 = C_{A0} - C_{A0}^d$, and $u_3 = T_{j10} - T_{j10}^d$, and three outputs: $y_1 = \mathbb{x}_{11}$, $y_2 = \mathbb{x}_{21}$ and $y_3 = \mathbb{x}_{31}$. Same as that for Example-I, we suppose the mathematical function in (46) is unknown to the designer, and noise exists in the sampled inputs random but bounded in $[-0.1,\ 0.1]$. The sampling time is $\Delta T = 0.1s$, and the delays are $\tau_{i1} = \tau_{i2} = \tau_{i3} = 20$, $i = 1,2,3$.

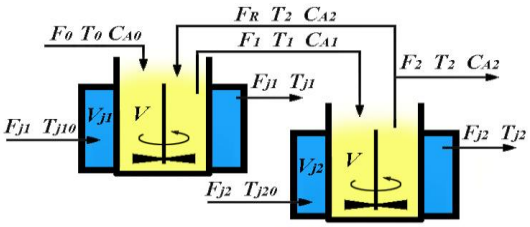


Fig. 9. Two continuous stirred-tank reactor

Table 3. Parameters of the continuous stirred-tank reactor in (46)

| | | |
|---|---|---|
| $\theta = 7.08 \times 10^{10}\ h^{-1}$ | $\rho = 800.9189\ kg/m^3$ | $T_0^d = 703.31$ ℃ |
| $E = 3.1644 \times 10^7\ J/mol$ | $\rho_j = 997.9450\ kg/m^3$ | $T_1^d = 665.9263$ ℃ |
| $R = 1679.2\ J/mol$℃ | $c_p = 1395.3\ J/kg$℃ | $T_2^d = 646.4508$ ℃ |
| $\delta = -3.1644 \times 10^7\ J/mol$ | $c_j = 1860.3\ J/kg$℃ | $T_{j1}^d = 740.8$ ℃ |
| $U = 1.3652 \times 10^6\ J/hm^2$℃ | $F = 2.8317\ m^3/h$ | $T_{j2}^d = 727.61$ ℃ |
| $C_{A0}^d = 18.368\ mol/m^3$ | $F_{j1} = 1.4130\ m^3/h$ | $V_j = 0.1090\ m^3$ |
| $C_{A1}^d = 12.305\ mol/m^3$ | $F_{j2} = 1.4130\ m^3/h$ | $V = 1.3592\ m^3$ |
| $C_{A2}^d = 18.3679\ mol/m^3$ | $F_R = 1.4158\ m^3/h$ | $A = 23.226\ m^2$ |
| $T_{j10}^d = 629.81$ ℃ | $T_{j20}^d = 608.29$ ℃ | $F_0 = 2.8317\ m^3/h$ |

Given the number of fuzzy rules as $L = 6$, the type-1 and type-2 T-S fuzzy models can be identified. Only the first rule is presented due to the limited pages:

*Rule* 1: If $x(k)$ is $\mathcal{X}^1$, Then
$y_1^1(k+1) = 0.7116y_1(k) + 0.0171y_1(k-1) + 0.1078u_1(k-20) - 3\times10^{-4}u_2(k-20) + 0.0676u_3(k-20)$
$y_2^1(k+1) = 1.6455y_2(k) - 0.6786y_2(k-1) + 0.0000\times u_1(k-20) + 0.0329u_2(k-20) + 0.0000\times u_3(k-20)$
$y_3^1(k+1) = 0.9728y_3(k) - 0.1697y_3(k-1) + 0.0160\,u_1(k-20) - 2\times10^{-5}u_2(k-20) + 0.0802u_3(k-20)$

where the center of $\mathcal{X}^1$ is $x_c^1 = [-5.2542\ \ 0.4564\ \ -1.8258\ \ -5.1538\ \ 0.4025\ \ -1.7947\ \ -12.7902\ \ 0.9987\ \ -2.1975]^T$, and $\Delta\mu^1 = 0.4966$ for the first type-2 fuzzy set. The comparisons between real outputs and fuzzy models' outputs with the RMSEs are shown in Fig. 10. The type-2 fuzzy model still gives smaller errors than its type-1 counterpart does.

During the data collection, $u_2$ has quite small impacts on $y_1$ and $y_3$, and the changes of $u_1$ or $u_3$ hardly influence $y_2$. These facts are also reflected by the coefficients of the fuzzy model that in the local models to calculate $y_1^l(k+1)$ and $y_3^l(k+1)$, the gains of $u_2$ are much smaller than that of $u_1$ and $u_3$, and in the local models to calculate $y_2^l(k+1)$, the gains of $u_1$ and $u_3$ are neighboring 0. Therefore, the channel $y_2 - u_2$ is of an extremely high degree of independence.

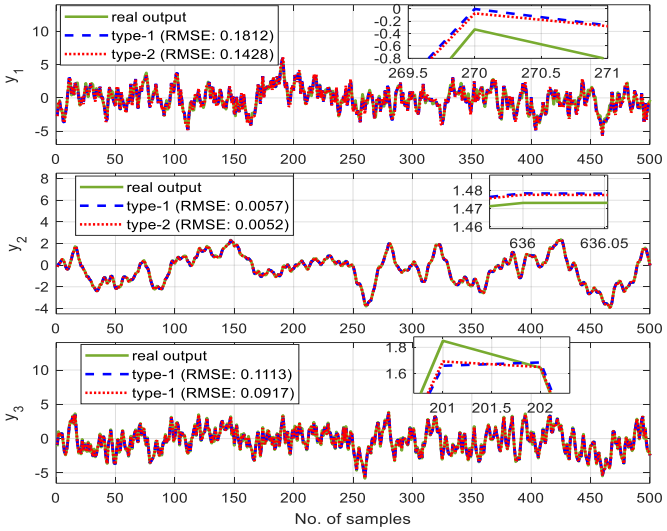


Fig. 10. Comparisons of real outputs and fuzzy models' outputs for (46)

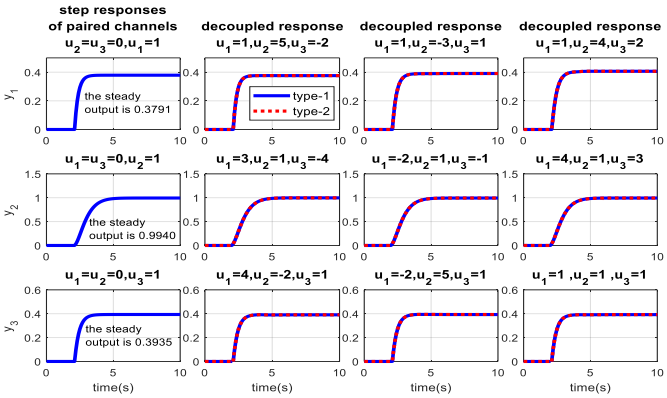


Fig. 11. The step responses of the three paired channels of (46)

We present $\mathcal{K}$, $\mathcal{E}$, RGA, and RNGA calculated from type-2 fuzzy model at $x(k) = [0\ \cdots 0]^T \in \mathbb{R}^9$ as an example:

$$\mathcal{K} = \begin{bmatrix} 0.3995 & 0.0001 & 0.2534 \\ 0 & 0.9902 & 0.0047 \\ 0.0847 & -0.0009 & 0.3954 \end{bmatrix}, \mathcal{E} = \begin{bmatrix} 2.3950 & 2.3950 & 2.3950 \\ 2.9740 & 2.9740 & 2.9740 \\ 2.3932 & 2.3932 & 2.3932 \end{bmatrix}$$

$$RGA = \begin{bmatrix} 1.1573 & 0.0000 & -0.1573 \\ 0.0000 & 1.0000 & 0.0000 \\ -0.1573 & 0.0000 & 1.1573 \end{bmatrix}$$

$$RNGA = \begin{bmatrix} 1.1573 & 0.0000 & -0.1573 \\ 0.0000 & 1.0000 & 0.0000 \\ -0.1573 & 0.0000 & 1.1573 \end{bmatrix}$$

The pairing structure is formed by the diagonal elements: $y_1 - u_1/y_2 - u_2/y_3 - u_3$, and then we have the following arrays:

$$\mathcal{A}_{Row} = \mathcal{A}_{Col} = \mathcal{B}_{Row} = \mathcal{B}_{Col} = \begin{bmatrix} 1.0000 & 0.0000 & 0.1359 \\ 0.0000 & 1.0000 & 0.0000 \\ 0.1359 & 0.0000 & 1.0000 \end{bmatrix}$$

Choosing $\varepsilon_\alpha = \varepsilon_\beta = 0.1$, the selected unpaired elements for sparse control are $y_1 - u_3$ and $y_3 - u_1$. Note that the calculated results from type-1 fuzzy model give the same pairing structure and select same unpaired elements. During the whole control

period, the pairing structure and sparse control structure for this MIMO system are unchanged.

A decoupling compensator is calculated using (38) for this MIMO system. Similar to that in Example-I, the step responses of isolated paired channels and the decoupled responses are compared and shown in Fig. 11. The decoupling compensator can largely reduce the coupling effects.

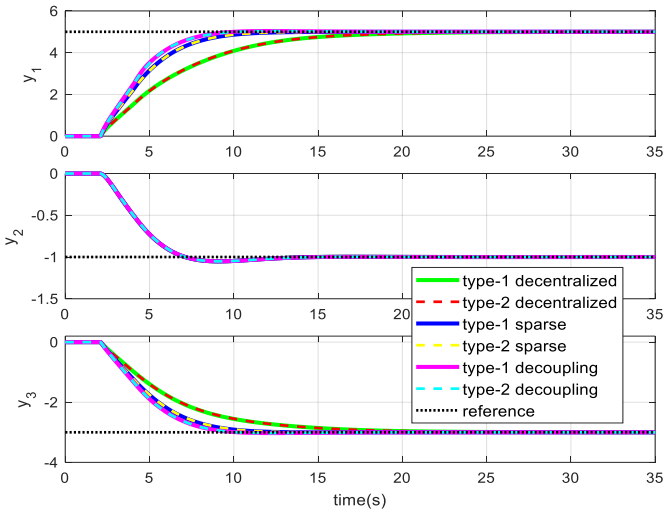


Fig. 12. Comparisons of three control strategies for the original system (46)

Table 4. The IAEs of the control performances in Fig. 12

| Controllers | $y_1$ | $y_2$ | $y_3$ |
|---|---|---|---|
| Type-1 decentralized | 34.1509 | 4.4643 | 19.4694 |
| Type-2 decentralized | 34.0791 | 4.4647 | 19.4163 |
| Type-1 sparse | 24.1940 | 4.4646 | 14.0118 |
| Type-2 sparse | 24.0616 | 4.4645 | 13.9777 |
| Type-1 decoupling | 22.3149 | 4.4644 | 13.2597 |
| Type-2 decoupling | 22.1747 | 4.4648 | 13.2253 |

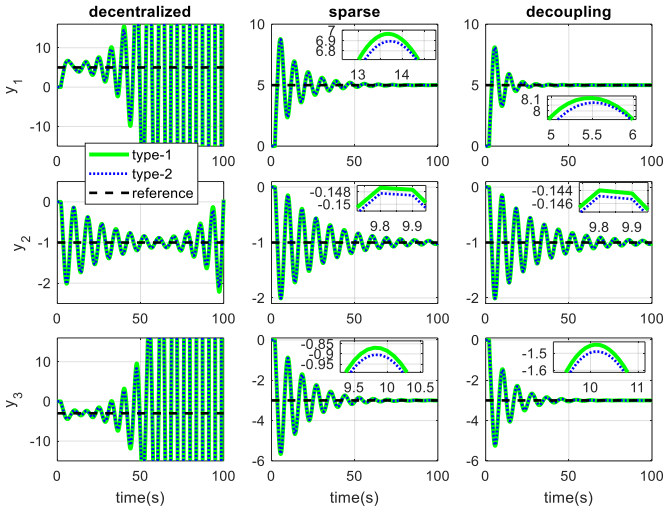


Fig. 13. Comparisons of three control strategies for Case-I of (46)

Given the references as $rv_1 = 5$, $rv_2 = -1$ and $rv_3 = -3$, the gain and phase margins based control algorithm using the same settings as that used in Example-I is applied to design the sub-controllers for decentralized, sparse and decoupling control systems. The performances of these control strategies for (46) are shown in Fig. 12 and Table 4. From Fig. 12, no evident overshoots can be found in the output responses. For $y_1$ and $y_3$, decoupling control achieves smallest setting time, which can be proved by the IAEs in Table 4. In this case, type-1 and type-2 fuzzy models have comparable performances.

Suppose the gains of the system inputs in (46) are enlarged due to the uncertainties to have the following two cases:

**Case-I**: the gains of three inputs become 3;

**Case-II**: the gains of $u_1$ and $u_3$ become 3.6, and the gain of $u_2$ is 3.

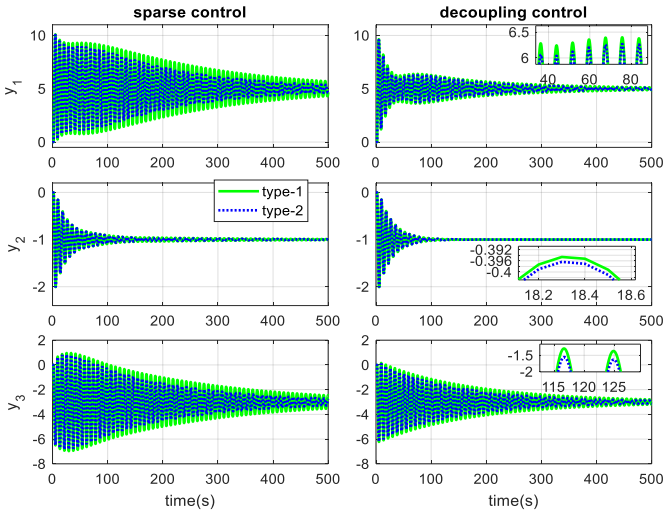


Fig. 14. Comparisons of three control strategies for Case-II of (46)

Table 5. The IAEs of the control performances in Figs. 13 and 14

| Cases | Controllers | $y_1$ | $y_2$ | $y_3$ |
|---|---|---|---|---|
| Case-I | Type-1 sparse | 51.5843 | 20.0265 | 40.7279 |
| | Type-2 sparse | 50.1289 | 19.9535 | 39.8654 |
| | Type-1 decoupling | 37.3054 | 20.0340 | 34.4712 |
| | Type-2 decoupling | 36.4807 | 20.0182 | 33.4763 |
| Case-II | Type-1 sparse | 859.3205 | 26.9938 | 671.8514 |
| | Type-2 sparse | 646.9325 | 26.8606 | 521.7338 |
| | Type-1 decoupling | 259.4291 | 20.9326 | 378.0959 |
| | Type-2 decoupling | 221.9645 | 20.9291 | 305.0214 |

The three controllers designed for the original MIMO system are applied to the revised systems of Case-I and Case-II to test their robustness as shown in Figs. 13-14 and Table 5. In Fig. 13 for Case-I, under the decentralized control, all the outputs, including $y_2$ become instable. The reason is that all the sub-controllers share the same fuzzy membership grades. Although $y_2 - u_2$ has a high degree of independence, the sub-controller for $y_2 - u_2$ using the fuzzy membership grades calculated from other instable outputs can cause $y_2$ to be divergent. Whereas the system is stable under both sparse and decoupling control. For $y_1$ and $y_3$, the decoupling control achieves better performance than the sparse control does in terms of overshoot, settling time and IAE. In Fig. 14 for Case-II, the decoupling control still achieves better results than the sparse control does. For the $y_2$ in Case-II, even the gain of $u_2$ is same as that in Case-I, its settling time under the sparse control is longer than that in Case-I because of the same reason mentioned before that all sub-controllers share the same fuzzy membership grades. From Figs. 13-14 and Table 5, type-2 fuzzy model results in smaller oscillation, settling period and IAE than its type-1 counterpart, which is more evident when the uncertainties become larger.

## VI. Conclusion

This paper presents a sparse control strategy and a decoupling control strategy based on type-1 and type-2 T-S fuzzy models to deal with the closely coupled effects in MIMO systems. Compared to the decentralized control strategy in [15], improvements are made on fuzzy modeling and ETSM calculation, such that the MIMO system dynamics can be expressed better and the coupling effects can be described more accurately. For the sparse control strategy, four indexes are defined from RNGA based criterion to select the sparse control structure, and an ETSM based approach is developed to convert the sparse controller design to a group of independent SISO controller designs. For the decoupling control strategy, a fuzzy model based decoupling compensator is proposed which is simple in calculation and easy to implement, and its stability, properness and causality can be guaranteed. The decoupling compensator can effectively reduce the steady and dynamic coupling effects such that the MIMO system can be regarded as multiple non-interacting SISO systems, which greatly offload the burden on decentralized controller design. The proposed two strategies offer the frameworks where linear SISO control algorithms can be directly utilized to manipulate the nonlinear MIMO systems with strongly coupled channels and without knowing the mathematical functions. The case studies demonstrate that both sparse and decoupling control outperform their decentralized counterpart, and decoupling control achieve better results than sparse control does. In addition, type-2 fuzzy model is more robust compared to its type-1 counterpart.

## References


[1] Q. Xiong, W.J. Cai, M.J. He, A practical loop pairing criterion for multivariable processes, *Journal of Process Control*, 15 (2005) 741-747.

[2] M.J. He, W.J. Cai, W. Ni, L.H. Xie, RNGA based control system configuration for multivariable processes, *Journal of Process Control*, 19 (2009) 1036-1042.

[3] Q.F. Liao, W.J. Cai, S.Y. Li, Y.Y. Wang, Interaction analysis and loop pairing for MIMO processes described by T-S fuzzy models, *Fuzzy Sets and Systems*, 207 (2012) 64-76.

[4] B. Wittenmark, M. E. Salgado, Hankel-norm based interaction measure for input-output pairing, *Proceedings of the 15th IFAC World Congress*, Barcelona, Spain, 2000.

[5] A. Conley, M. E. Salgado, MIMO interaction measure and controller structure selection, *International Journal of Control*, 77 (2004) 367-383.

[6] H. R. Shaker, J. Stoustrup, An interaction measure for control configuration selection for multivariable bilinear systems, *Nonlinear Dynamics*, 72 (2013) 165-174.

[7] H. R. Shaker, M. Komareji, Control configuration selection for multivariable nonlinear systems, *Industrial and Engineering Chemistry Research*, 51 (2012) 8583-8587.

[8] E.H. Bristol, On a new measure of interaction for multi-variable process control, *IEEE Transactions on Automatic Control*, 11(1966) 133-134.

[9] M. Witcher, T.J. McAvoy, Interacting control systems: steady state and dynamic measurement of interaction, *ISA Transactions*, 16 (1977) 83-90.

[10] T. McAvoy, Y. Arkun, R. Chen, D. Robinson, P.D. Schnelle, A new approach to defining a dynamic relative gain, *Control Engineering Practice*, 11 (2003) 907-914.

[11] Q.F. Liao, D. Sun, Interaction measures for control configuration selection based on interval type-2 Takagi-Sugeno fuzzy model, *IEEE Transactions on Fuzzy Systems* (2018).

[12] H.P. Huang, J.C. Jeng, C.H. Chiang, W. Pan, A direct method for multi-loop PI/PID controller design, *Journal of Process Control* 13(2003) 769-786.

[13] Q. Xiong, W.J. Cai, Effective transfer function method for decentralized control system design of multi-input multi-output processes, *Journal of Process Control* 16(2006) 773-784.

[14] Y.L. Shen, W.J. Cai, S.Y. Li, Multivariable process control: decentralized, decoupling, or sparse? *Industrial & Engineering Chemistry Research* 49 (2010) 761-771.

[15] Q.F. Liao, D. Sun, W.J. Cai, S.Y. Li, Y.Y. Wang, Type-1 and Type-2 effective Takagi-Sugeno fuzzy models for decentralized control of multi-input-multi-output processes, *Journal of Process Control* 52 (2017) 26-44.

[16] Y. Hao, General SISO Takagi-Sugeno fuzzy systems with linear rule consequent are universal approximators, *IEEE Transactions on Fuzzy Systems* 6 (1998) 582-587

[17] J. Lee, D.H. Kim, T.F. Edgar, Static decouplers for control of multivariable processes, *AIChE Journal* 51(2005), 2712-2720.

[18] S. Tavakoli, I. Griffin, P.J. Fleming, Tuning of decentralised PI (PID) controllers for TITO processes, *Control Engineering Practice* 14(2006) 1069-1080

[19] B.T. Jevtović, M.R. Mataušek, PID controller design of TITO system based on ideal decoupler, *Journal of Process Control* 20(2010) 869-876

[20] J. Garrido, F. Vázquez, F. Morilla, Centralized multivariable control by simplified decoupling, *Journal of Process Control* 22(2012) 1044-1062

[21] W. J. Cai, W. Ni, M.J. He, C.Y. Ni, Normalized decoupling–A new approach for MIMO process control system design, *Industrial and Engineering Chemistry Research*, 47(2008) 7347-7356.

[22] Y. Jiang, Y. Zhu, K. Yang, C. Hu, D. Yu, A Data-Driven Iterative Decoupling Feedforward Control Strategy With Application to an Ultraprecision Motion Stage, *IEEE Transactions on Industrial Electronics* 62(2015) 620-627

[23] J. Garridoa, F. Vázqueza, F. Morilla, Inverted decoupling internal model control for square stable multivariable time delay systems, *Journal of Process Control* 24(2014) 1710-1719.

[24] C. Wang, W. Zhao, Z. Luan, Q. Gao, K. Deng, Decoupling control of vehicle chassis system based on neural network inverse system, *Mechanical Systems and Signal Processing* 106 (2018) 176-197

[25] H. Zhou, H. Deng, J. Duan, Hybrid Fuzzy Decoupling Control for a Precision Maglev Motion System, 23 (2018) 389-401

[26] Y. Zhang, T, Chai, H. Wang, D, Wang, X. Chen, Nonlinear Decoupling Control With ANFIS-Based Unmodeled Dynamics Compensation for a Class of Complex Industrial Processes *IEEE Transactions on Neural Networks And Learning Systems* 29(2018) 2352-2366

[27] M. Wu, J. Yan, J-H. She, W-H. Cao, Intelligent Decoupling Control of Gas Collection Process of Multiple Asymmetric Coke Ovens, *IEEE Transactions on Industrial Electronics* 56(2009) 2782-2792

[28] G. Feng, A survey on analysis and design of model-Based fuzzy control systems, *IEEE Transactions on Fuzzy Systems* 14 (2006) 676-697.

[29] Q.L. Liang, J.M. Mendel, An introduction to type-2 TSK fuzzy logic systems, *IEEE International Fuzzy Systems. Conference Proceedings*, Seoul, South Korea, 1999, pp. 1534-1539

[30] N.N. Karnik, J.M. Mendel, Q.L Liang, Type-2 fuzzy logic systems, *IEEE Transactions on Fuzzy Systems*, 7 (1999) 643-658

[31] D. Sun, Q. Liao, and H. Ren, Type-2 fuzzy logic based time-delayed shared control in online-switching tele-operated and autonomous systems, *Robotics and Autonomous Systems*, 101 (2018) 138–152.

[32] D. Sun, Q. Liao, and H. Ren, Type-2 fuzzy modeling and control for bilateral teleoperation system with dynamic uncertainties and timevarying delays, *IEEE Transactions on Industrial Electronics*, 65(2018) 447–459.

[33] D. Sun, Q. Liao, X. Gu, C. Li, H. Ren, Multilateral Teleoperation with New Cooperative Structure Based on Reconfigurable Robots and Type-2 Fuzzy Logic, *IEEE Transactions on Cybernetics*, 2018.

[34] A. Niederlinski, A heuristic approach to the design of linear multivariable interacting subsystems, *Automatica* 7 (1971) 691-701

[35] B. Chen, X.P. Liu, K.F. Liu, C. Lin, Adaptive fuzzy tracking control of nonlinear MIMO systems with time-varying delays, *Fuzzy Sets and Systems*, 217 (2013) 1-21.

**Qianfang Liao** received the B.Eng. degree in Automation from Wuhan University, China, in 2006, the M.Eng. degree in Automation from Shanghai Jiao Tong University, China, in 2009, and the Ph.D. degree from the School of Electrical and Electronic Engineering, Nanyang Technological University, Singapore, in 2015. From 2015 to 2017, she was a Research Fellow with Nanyang Technological University and National University of Singapore, Singapore. She is currently a Researcher with Örebro University, Sweden. Her current research interests include fuzzy modeling, control theory, and machine learning.

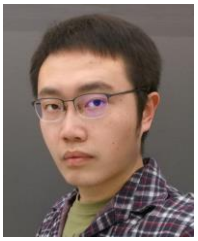

**Da Sun** received the B.Eng. and Ph.D. degrees in Mechatronics from University of Wollongong, Wollongong, Australia, in 2012 and 2016, respectively. In 2016, He also received Chinese Government Award for outstanding self-financed students abroad. From 2016 to 2017, he was a Research Fellow with National University of Singapore, Singapore. From 2017 to now, he is a Researcher with Örebro University, Sweden. His current research interest includes robotics learning, control theory, teleoperation, and virtual reality.